

## Stochastic Toda-oscillator model of the bad-cavity laser

Tetsuo Ogawa\*

*Department of Applied Physics, Faculty of Engineering, The University of Tokyo, 7-3-1 Hongo, Bunkyo-ku, Tokyo 113, Japan*

(Received 12 March 1990)

The statistical noise properties of the laser radiation in a low- $Q$  (bad) cavity are theoretically investigated. The bad-cavity laser system is shown to be exactly equivalent to the *stochastic Toda oscillator* (STO) in the case of negligible polarization noise. Transforming the STO Langevin equation to the Fokker-Planck equation with a position-dependent diffusion coefficient, analytical expressions of the probability distribution are obtained as particular solutions in a stationary state with the aid of the expansion into a complete orthogonal set. We predict novel statistical features of the laser light, e.g., a power tail of the intensity distribution function, non-Gaussian nature of the field fluctuation, and super-Poissonian photoelectron statistics. General solutions are also given in a closed form in terms of the matrix continued fraction to compare with the particular solutions. The good-cavity case is reanalyzed in our formalism to root out differences between them.

### I. INTRODUCTION

Statistical dynamics of lasers have been investigated very much in terms of nonequilibrium and nonlinear statistical physics.<sup>1,2</sup> Lasers are a good example of a nonlinear stochastic system that has increased current interest not only in fundamental physics but also in the wide field of applications of lasers. The information transmission rates in optical communications, the accuracy of optical computing techniques, and the reliability of spectroscopic data are dependent on and limited by the nature of the fluctuations present in the laser light.

The Langevin equations and/or the Fokker-Planck equations (FPE's) of laser variables have been tried to be solved in order to clarify the statistical feature of lasers, particularly multimode dye lasers. The dynamics of lasers with two-level materials is essentially characterized by three relaxation constants in the semiclassical model: the field decay rate  $K$ , including a transmission loss through the cavity mirrors, the polarization relaxation constant (the transverse decay rate)  $\gamma_{\perp}$ , and the population relaxation constant (the longitudinal decay rate)  $\gamma_{\parallel}$ . So far, lasers with a high- $Q$  cavity (under the good-cavity condition) have been given much attention because their condition is more easily accessible in experiments. In the limit of  $K \ll \gamma_{\parallel}, \gamma_{\perp}$ , the simplest model, the one-variable Langevin equation, was employed and analyzed.<sup>3</sup> The adiabatic elimination of both the polarization and population difference is valid in this limit. In the case of  $K, \gamma_{\parallel} \ll \gamma_{\perp}$ , however, both the electric field and population need to be considered, and the adiabatic approximation is justified only for the polarization. As a result, multivariable FPE must be treated.<sup>4</sup> In this case, the detailed balance is violated and it is harder to get stationary solutions of the FPE than in the one-variable case. Recently, a CO<sub>2</sub> laser has been studied in the limit of  $\gamma_{\parallel} \ll K, \gamma_{\perp}$  with the aid of the center manifold theorem.<sup>5</sup>

A laser with a low- $Q$  cavity (under the bad-cavity con-

dition  $K > \gamma_{\parallel}, \gamma_{\perp}$ ), on the other hand, is also an interesting system in terms of its strong dissipation and nonlinearity from the viewpoint of statistical physics. In this system, we need to consider both the atomic polarization and population difference to discuss the laser dynamics by eliminating the electric field only.<sup>6,7</sup> Experimental studies on this system have recently progressed by the use of far-infrared (FIR) lasers and masers.<sup>8</sup> However, thus far there has been little progress in the theoretical understanding of this bad-cavity system. Deterministic modulation properties of this system were comprehensively clarified in terms of optical chaos and bifurcation sequences.<sup>9,10</sup> The modulated system is equivalent to the *forced* Toda oscillator and exhibits a variety of deterministic dynamics including bistability, nonlinear resonance, quasiperiodicity, and intermittent behavior. In this paper, on the other hand, we pay attention to the stochastic dynamics of the laser with a low- $Q$  cavity described by the Langevin equation of the *stochastic* Toda oscillator (STO), and the resultant two-variable FPE is analytically solved for the first time to clarify the statistical properties of the radiation under the bad-cavity condition. It is so difficult to obtain the steady-state solutions of the two-variable FPE because of the violation of the detailed balance that many problems remain to be solved.

In our preceding Rapid Communication,<sup>11</sup> we reported briefly analytic solutions of the FPE for the STO model and derived a novel intensity distribution function with a longer tail than that in the good-cavity case. More detailed results are reported in this paper. The way both the deterministic and statistical dynamics of laser radiation depend on the number of operating longitudinal modes is also interesting. In accordance with its number, we must use a proper model to describe lasers. (i) In the single-mode operation, a laser becomes a low-dimensional dynamical system if fluctuations are negligible, which has been studied in terms of optical chaos and Lorenz insta-

bility.<sup>12</sup> (ii) When several longitudinal modes oscillate simultaneously, on the other hand, the system has many degrees of freedom which require the high-dimensional model. In this case, numerical analysis becomes a powerful tool instead of analytical methods to study the high-dimensional properties of deterministic dynamics.<sup>13,14</sup> (iii) In particular, when infinitely many modes operate simultaneously as in a dye laser, stochastic forces can be employed to describe phenomenologically the fluctuation effects of the many off-resonant modes on the relevant resonant mode.<sup>15</sup> This is also one approach to clarify the statistics of optical multimode chaos found under the bad-cavity condition.<sup>14</sup> In this way, the stochastic model may also describe a limit of a many multimode operation of a deterministic laser. The stochastic and deterministic (dynamical) approaches are complements of each other in the study of multimode operation. However, we should note that the central limit theorem cannot be applied to the multimode laser because modes are not independent of one another and the mode-mode interaction plays an important role in multimode laser fluctuations.<sup>16</sup>

This paper is concerned with the bad-cavity laser with field and population fluctuations. No polarization fluctuation is considered and it is shown to be negligible, e.g., in the strong pumping case. The case where the polarization fluctuation is also considered in addition to the field and population noises has already been investigated in detail in Refs. 6 and 7 with the use of other methods. Comparison between them will be made afterwards. Concerning a bad-cavity property, laser Langevin equations contain not only additive noises but also multiplicative ones resulting from the adiabatic elimination of the field. We transform them to the STO Langevin equation by a logarithmic transformation and to the two-dimensional FPE which is similar to the one-dimensional Kramers equation, but is different in a diffusion coefficient depending on a position variable. We seek analytic solutions of the FPE as particular solutions in the stationary state with the aid of an expansion method into a complete orthogonal set (a kind of eigenfunction expansion). These are exact solutions in the case where the field noise is weak; otherwise, we obtain approximate solutions yielding a *power tail* of the intensity distribution function.<sup>11</sup> Novel statistical features of the laser light which result from its longer tail are predicted for the first time. The stationary intensity variance and photoelectron statistics are paid particular attention to clarify the non-Gaussian and the super-Poissonian characteristics. In addition, general solutions are also given in a closed form in terms of the matrix continued fraction<sup>17</sup> (MCF). Comparison between the particular solutions and general MCF ones are made to discuss the velocity distribution function of the STO. The good-cavity case is also reanalyzed in our formalism to derive the modified STO equation and to root out differences from the bad-cavity case. These results will become foundations in applying the low- $Q$  cavity laser to optical communications, optical information processing, and incoherent laser spectroscopy, and in analyzing the cavityless laser or the amplified spontaneous emission.

This paper is organized as follows. In Sec. II the stochastic Toda-oscillator model is introduced and the

relevant FPE is derived. The probability density of the Toda-oscillator variables is expanded to the orthogonal complete set. Under a suitable “no-current” condition, we obtain in Sec. III analytic solutions of FPE and discuss the intensity statistics and photoelectron statistics. A general solution is given in Sec. IV to discuss the population (velocity) distribution function. For comparison, the good-cavity case is reexamined in Sec. V. Discussion on the pseudoenergy and stability of the STO and a summary are given in Sec. VI.

## II. STOCHASTIC TODA-OSCILLATOR MODEL

### A. Langevin Maxwell-Bloch equations

The interaction of the cavity field with the two-level material is described *semiclassically* by the Maxwell-Bloch equations of the electric field envelope  $E$ , the polarization envelope  $P$ , and the population difference  $D$  in the slowly varying approximation. The field is assumed to be a plane wave and no spatial structure is considered throughout this paper. We shall consider three kinds of *classical* fluctuating forces: the field noise  $\Gamma_E(t) \equiv \Gamma_1(t) + i\Gamma_2(t)$ , the polarization noise  $\Gamma_P(t) \equiv \Gamma_3(t) + i\Gamma_4(t)$ , and the population noise  $\Gamma_D(t) \equiv \Gamma_5(t)$ , which are applied, respectively, to each variable. Here the  $\Gamma_j(t)$ 's ( $j = 1, \dots, 5$ ) are real. Then we start with the Langevin Maxwell-Bloch equations in the case of atomic resonance under the mean-field approximation

$$\frac{d}{dt}E(t) = -KE + igP + \left[ \frac{\mathcal{S}_E}{4} \right]^{1/2} \Gamma_E(t), \quad (2.1a)$$

$$\frac{d}{dt}P(t) = -\gamma_{\perp}P - igED + \left[ \frac{\mathcal{S}_P}{4} \right]^{1/2} \Gamma_P(t), \quad (2.1b)$$

$$\begin{aligned} \frac{d}{dt}D(t) = & -\gamma_{\parallel}D + \gamma_{\parallel}D^{(0)} + 2ig(EP^* - E^*P) \\ & + \left[ \frac{\mathcal{S}_D}{2} \right]^{1/2} \Gamma_D(t), \end{aligned} \quad (2.1c)$$

where  $g$  is a coupling constant between field and matter, and  $D^{(0)}$  denotes the population inversion describing a pumping. Here  $\mathcal{S}_E$ ,  $\mathcal{S}_P$ , and  $\mathcal{S}_D$  are measures of fluctuation strength, which should be simply determined by the fluctuation-dissipation theorem in the semiclassical single-mode laser system.<sup>4,5,17,18</sup> Multimode effects are also included in  $\mathcal{S}_E$ ,  $\mathcal{S}_P$ , and  $\mathcal{S}_D$  as additional terms  $\mathcal{S}_E^{\text{ex}}$ ,  $\mathcal{S}_P^{\text{ex}}$ , and  $\mathcal{S}_D^{\text{ex}}$ , respectively. Therefore, we treat them as control parameters, i.e.,

$$\mathcal{S}_E = 2Kn_{\text{th}} + \mathcal{S}_E^{\text{ex}}, \quad (2.2a)$$

$$\mathcal{S}_P = 2\gamma_{\perp}N_2 + \mathcal{S}_P^{\text{ex}}, \quad (2.2b)$$

$$\mathcal{S}_D = 2\gamma_{\parallel}N + \mathcal{S}_D^{\text{ex}}, \quad (2.2c)$$

where  $n_{\text{th}} = [\exp(\hbar\omega_c/k_B T) - 1]^{-1}$  is the number of thermal photons (which is small in an optical frequency region) when the reservoir is in the thermal equilibrium with temperature  $T$ . An additional term  $\mathcal{S}_E^{\text{ex}}$  represents

extrinsic contributions to the field noise, e.g., the off-resonant mode fluctuations or an injected noise field. The polarization noise strength  $\mathcal{S}_P$  is derived to satisfy Einstein's theory and includes the population of the upper atomic level  $N_2$ . The total population is denoted as  $N$ . Although  $N_2$  depends on  $D(t)$  in a strict sense (i.e.,  $N_2 = N_2(t) = \frac{1}{2}[N + D(t)]$ ), we assume in this paper that  $\mathcal{S}$ ,  $N_2$ , and  $N$  are constant in time for simplicity. The extrinsic population noises (including a pump noise and multimode effects) are described in  $\mathcal{S}_D^{\text{ex}}$ , which is assumed to be a small constant independent of a pump parameter.<sup>19</sup>

In the case of a low- $Q$  cavity, the electric field follows adiabatically the material variables. Then, eliminating  $E(t)$  from Eq. (2.1), we get

$$\begin{aligned} \frac{d}{dt}P(t) = & -\gamma_{\perp}P + \frac{g^2}{K}PD - i\frac{g}{K}\left[\frac{\mathcal{S}_E}{4}\right]^{1/2}D\Gamma_E(t) \\ & + \left[\frac{\mathcal{S}_P}{4}\right]^{1/2}\Gamma_P(t), \end{aligned} \quad (2.3a)$$

$$\begin{aligned} \frac{d}{dt}D(t) = & -\gamma_{\parallel}D + \gamma_{\parallel}D^{(0)} - 4\frac{g^2}{K}|P|^2 \\ & + \left[\frac{\mathcal{S}_D}{2}\right]^{1/2}\Gamma_D(t) \\ & - 4\frac{g}{K}\left[\frac{\mathcal{S}_E}{4}\right]^{1/2}\text{Im}[P^*\Gamma_E(t)]. \end{aligned} \quad (2.3b)$$

Because of this adiabatic elimination procedure,<sup>20</sup> not only additive fluctuation terms but also multiplicative ones appear in the Langevin equations [Eqs. (2.3)]. Here we shall use normalized variables in dimensionless units:

$$\tau \equiv \gamma_{\perp}t, \quad (2.4a)$$

$$\bar{P}(\tau) \equiv \frac{2g^2}{K(\bar{A}\gamma_{\perp}\gamma_{\parallel})^{1/2}}P(\tau), \quad (2.4b)$$

$$\bar{D}(\tau) \equiv \frac{D(\tau)}{D_{\text{th}}}, \quad (2.4c)$$

where  $D_{\text{th}} \equiv K\gamma_{\perp}/g^2$  is a lasing threshold of the population inversion, and  $\bar{A} \equiv D^{(0)}/D_{\text{th}} - 1$  is a pump parameter which is zero at threshold. In the noiseless (deterministic) case ( $\mathcal{S}_E = \mathcal{S}_P = \mathcal{S}_D = 0$ ),  $|\bar{P}|$  and  $\bar{D}$  become unity in the steady state above the threshold ( $\bar{A} > 0$ ). Then the Langevin equations become

$$\begin{aligned} \frac{d}{d\tau}\bar{P}(\tau) = & \bar{P}(\bar{D} - 1) - i\frac{\bar{D}}{2}\left[\frac{\mathcal{S}_E}{\gamma\bar{A}}\right]^{1/2}\Gamma_E(\tau) \\ & + \frac{1}{2}\left[\frac{\mathcal{S}_P}{\gamma\bar{A}}\right]^{1/2}\Gamma_P(\tau), \end{aligned} \quad (2.5a)$$

$$\begin{aligned} \frac{d}{d\tau}\bar{D}(\tau) = & -\gamma\bar{D} + \gamma(\bar{A} + 1) - \gamma\bar{A}|\bar{P}|^2 \\ & + (\gamma\mathcal{S}_D)^{1/2}\Gamma_D(\tau) \\ & - \frac{1}{2}(\gamma\bar{A}\mathcal{S}_E)^{1/2}\text{Im}[\bar{P}^*\Gamma_E(\tau)]. \end{aligned} \quad (2.5b)$$

The ratio  $\gamma = \gamma_{\parallel}/\gamma_{\perp}$  is restricted to be less than 2 and is small in an ordinary lasing medium. The noise strengths are rewritten for simplicity by three control parameters independent of  $\bar{A}$  as

$$S_E = \left[\frac{2}{gD_{\text{th}}}\right]^2 \mathcal{S}_E, \quad (2.6a)$$

$$S_P = \left[\frac{2}{\gamma_{\perp}D_{\text{th}}}\right]^2 \mathcal{S}_P, \quad (2.6b)$$

$$S_D = \frac{1}{2\gamma} \left[\frac{1}{\gamma_{\perp}D_{\text{th}}}\right]^2 \mathcal{S}_D. \quad (2.6c)$$

Here we confine our discussion to the case where the pumping is rather strong ( $\bar{A} > 1$ ) and fluctuating forces applied on  $\bar{P}$  are negligible in comparison with those on  $\bar{D}$ . Then the phase of polarization  $\varphi \equiv \arg\bar{P}$  is nearly constant in time ( $d\varphi/d\tau \simeq 0$ ). Thus we consider the situation in which  $\Gamma_E(\tau)$  and  $\Gamma_D(\tau)$  play dominant roles as the fluctuations on the population difference of the system. Eliminating  $\bar{D}(\tau)$  from Eqs. (2.5) in an exact manner, the second-order stochastic differential equation of  $\bar{P}(\tau)$  is derived. Additionally, employing the logarithmic transform,<sup>9</sup> i.e.,

$$u(\tau) \equiv 2 \ln|\bar{P}(\tau)|, \quad (2.7)$$

we arrive at the STO equation

$$\begin{aligned} \frac{d^2u}{d\tau^2} + \gamma\frac{du}{d\tau} + 2\gamma\bar{A}\frac{dU(u)}{du} \\ = 2(\gamma\mathcal{S}_D)^{1/2}\Gamma_5(\tau) + (\gamma\bar{A}\mathcal{S}_E)^{1/2}e^{u/2}\sin\varphi\Gamma_1(\tau) \\ - (\gamma\bar{A}\mathcal{S}_E)^{1/2}e^{u/2}\cos\varphi\Gamma_2(\tau), \end{aligned} \quad (2.8)$$

where

$$U(u) \equiv e^u - u - 1 \quad (2.9)$$

is the Toda potential which is an asymmetric potential. Here  $\gamma$  plays as a damping constant of the STO and  $-2\gamma\bar{A}dU/du$  is the force due to the potential. The variables  $u(\tau)$  and  $\dot{u}(\tau) \equiv du(\tau)/d\tau$  describe the position and velocity of the Brownian particle, respectively, bounded in the potential  $2\gamma\bar{A}U(u)$  and applied the fluctuating forces. A position-independent friction  $\gamma\dot{u}$  and a position-dependent fluctuation (corresponding to the  $u$ -dependent temperature)  $e^{u/2}\Gamma_i(\tau)$  are characteristics of the STO system describing the bad-cavity laser. The readers should compare with the modified STO equation [Eq. (5.1)] in the good-cavity case (Sec. V A).

## B. Fokker-Planck equation for the STO

We consider the case where the correlation times of the noises are much smaller than the fastest characteristic time of the dynamical system  $\sim K^{-1}$ . Therefore, in the first approximation, the fluctuations  $\Gamma_i(\tau)$ 's are assumed to be the Gaussian random processes with zero means and  $\delta$  correlations, i.e.,

$$\langle \Gamma_i(\tau) \rangle = 0, \quad (2.10a)$$

$$\langle \Gamma_i(\tau) \Gamma_j(\tau') \rangle = 2\delta_{ij} \delta(\tau - \tau') \quad (i, j = 1, \dots, 5). \quad (2.10b)$$

In this case, the Langevin equations for two variables  $u$  and  $\dot{u}$  lead to the two-variable FPE:

$$\frac{\partial W(u, \dot{u}, \tau)}{\partial \tau} = \mathcal{L}_{\text{FP}}(u, \dot{u}) W(u, \dot{u}, \tau). \quad (2.11)$$

In Eq. (2.11),  $W(u, \dot{u}, \tau)$  is the distribution function in position and velocity space  $(u, \dot{u})$ . Here we note that  $u$  and  $\dot{u}$  are *independent* stochastic variables. The Fokker-Planck operator can be split into a reversible (streaming) part  $\mathcal{L}_{\text{rev}}$  and an irreversible (collision) part  $\mathcal{L}_{\text{irr}}$  as<sup>17</sup>

$$\mathcal{L}_{\text{FP}}(u, \dot{u}) = \mathcal{L}_{\text{rev}}(u, \dot{u}) + \mathcal{L}_{\text{irr}}(u, \dot{u}), \quad (2.12)$$

where

$$\mathcal{L}_{\text{rev}}(u, \dot{u}) \equiv -\dot{u} \frac{\partial}{\partial u} + 2\gamma \bar{A} \left[ \frac{dU(u)}{du} \right] \frac{\partial}{\partial \dot{u}}, \quad (2.13a)$$

$$\mathcal{L}_{\text{irr}}(u, \dot{u}) \equiv \gamma \frac{\partial}{\partial \dot{u}} \left[ \dot{u} + v_d^2(u) \frac{\partial}{\partial \dot{u}} \right]. \quad (2.13b)$$

The reversible operator describes the motion of an ensemble obeying the reversible equation,  $\ddot{u} = -2\gamma \bar{A} dU/du$ , and is shown to be an anti-Hermitian operator. The irreversible operator, which describes energy-dissipation through friction and diffusion, has a second-order derivative. This is neither an anti-Hermitian nor a Hermitian operator.

Equation (2.11) resembles the one-dimensional Kramers equation,<sup>21</sup> which is a special FPE describing the Brownian motion in a potential. The Kramers equation has been employed to study reaction kinetics, superionic conductors, Josephson tunneling junction, relaxation of dipoles, or second-order phase-locked loops. Here we find that in addition to above systems, the noisy bad-cavity laser is also described by a kind of Kramers equation. Risken<sup>17</sup> derived a general solution of the Kramers equation in terms of MCF for arbitrary potentials. Here we pay attention to a difference between our FPE for the STO and the original Kramers equation. The difference lies in the diffusion coefficient which depends on the position variable  $u$ , i.e.,

$$\gamma v_d^2(u) \equiv \gamma (\bar{A} S_E e^u + 4S_D), \quad (2.14)$$

in our FPE system, while the diffusion in the original Kramers equation is constant in position. This means that the thermal velocity (diffusion velocity) of the Brownian particle is a function of the position; that is, the temperature of environment depends on the position. In the  $u > 0$  region (corresponding to high intensity of laser light), the diffusion is stronger and the system suffers from the stronger noises. Position dependence of the diffusion makes it harder to solve the FPE.

Solving the FPE with the aid of the expansion into a complete orthogonal set, we seek, first of all, the most suitable set for the expansion. A stationary solution of  $\mathcal{L}_{\text{irr}}$  is proportional to  $\exp\{-\frac{1}{2}(\dot{u})^2/[2v_d^2(u)]\}$ . Therefore, by multiplying  $\mathcal{L}_{\text{irr}}$  from the left with a square root of the

stationary solution and from the right with its inverse,  $\mathcal{L}_{\text{irr}}$  can be brought to an Hermitian form, i.e.,

$$\begin{aligned} \mathcal{L}_{\text{irr}}^H &= \exp\left[\frac{(\dot{u})^2}{4v_d^2(u)}\right] \mathcal{L}_{\text{irr}} \exp\left[-\frac{(\dot{u})^2}{4v_d^2(u)}\right] \\ &= -\gamma a^\dagger a, \end{aligned} \quad (2.15)$$

where  $a$  ( $a^\dagger$ ) is the annihilation (creation) operator,

$$a = v_d(u) \frac{\partial}{\partial \dot{u}} + \frac{1}{2} \frac{\dot{u}}{v_d(u)}, \quad (2.16a)$$

$$a^\dagger = -v_d(u) \frac{\partial}{\partial \dot{u}} + \frac{1}{2} \frac{\dot{u}}{v_d(u)}. \quad (2.16b)$$

These satisfy a commutation relation for boson operators,  $[a, a^\dagger] = 1$ . For the reversible operator, we carry out the similar transform to get

$$\mathcal{L}_{\text{rev}}^H = -a D_1 - a^\dagger D_2 - \mathcal{L}_{\text{res}}. \quad (2.17)$$

Here we employ the differential operators  $D_1$  and  $D_2$ , defined by

$$D_1 = v_d(u) \frac{\partial}{\partial u}, \quad (2.18a)$$

$$D_2 = v_d(u) \frac{\partial}{\partial u} + \frac{2\gamma \bar{A}}{v_d(u)} \frac{dU(u)}{du}, \quad (2.18b)$$

and a residual part

$$\mathcal{L}_{\text{res}} = \frac{(\dot{u})^3}{2v_d^3(u)} \frac{dv_d(u)}{du}, \quad (2.19)$$

which results from the position dependence of the diffusion velocity.

Considering the natural boundary conditions,

$$\lim_{u \rightarrow \pm\infty} W(u, \dot{u}, \tau) = \lim_{\dot{u} \rightarrow \pm\infty} W(u, \dot{u}, \tau) = 0, \quad (2.20)$$

and the Fokker-Planck operator of the form

$$\begin{aligned} \mathcal{L}_{\text{FP}}(u, \dot{u}) &= -\Psi_0(\dot{u}; u) (\gamma a^\dagger a + a D_1 + a^\dagger D_2 + \mathcal{L}_{\text{res}}) \\ &\quad \times [\Psi_0(\dot{u}; u)]^{-1}, \end{aligned} \quad (2.21)$$

the probability distribution  $W$  is expanded with respect to  $\dot{u}$  is

$$W(u, \dot{u}, \tau) = \Psi_0(\dot{u}; u) \sum_{n=0}^{\infty} c_n(u, \tau) \Psi_n(\dot{u}; u), \quad (2.22)$$

where the expansion function is chosen to be the Hermite function as

$$\begin{aligned} \Psi_n(\dot{u}; u) &= \frac{1}{[n! \sqrt{2\pi} v_d(u)]^{1/2}} \\ &\quad \times \exp\left[-\frac{(\dot{u})^2}{4v_d^2(u)}\right] H_n\left[\frac{\dot{u}}{v_d(u)}\right]. \end{aligned} \quad (2.23)$$

Here  $H_n(x)$  is the Hermite polynomials defined by

$$H_n(z) = (-1)^n \exp\left[\frac{z^2}{2}\right] \frac{d^n}{dz^n} \exp\left[-\frac{z^2}{2}\right]. \quad (2.24)$$

The expansion functions  $\Psi_n(\dot{u}; u)$  ( $n=0, 1, 2, \dots$ ) form a complete set and have the correct natural boundary condition. They are eigenfunctions of  $\mathcal{L}_{\text{irr}}^H$ , that is,

$$\begin{aligned} \mathcal{L}_{\text{irr}}^H \Psi_n(\dot{u}; u) &= -\gamma a^\dagger a \Psi_n(\dot{u}; u) \\ &= -\gamma n \Psi_n(\dot{u}; u). \end{aligned} \quad (2.25)$$

Using the orthonormal relation,

$$\int_{-\infty}^{\infty} \Psi_m(\dot{u}; u) \Psi_n(\dot{u}; u) d\dot{u} = \delta_{mn}, \quad (2.26)$$

we obtain the one-sided recurrence equation for the expansion coefficients  $c_n(u, \tau)$  ( $n=0, 1, 2, \dots$ ), that is

$$\begin{aligned} \frac{\partial c_n(u, \tau)}{\partial \tau} &= \hat{f}_n^{(-3)} c_{n-3} + \hat{f}_n^{(-1)} c_{n-1} \\ &\quad + \hat{f}_n^{(0)} c_n + \hat{f}_n^{(1)} c_{n+1}, \end{aligned} \quad (2.27)$$

where  $c_n(u, \tau) = 0$  for  $n < 0$  and  $\hat{f}_n^{(k)}$ 's are the expansion-coefficient operators with respect to  $u$ :

$$\hat{f}_n^{(-3)} = -[n(n-1)(n-2)]^{1/2} \frac{dv_d(u)}{du}, \quad (2.28a)$$

$$\begin{aligned} \hat{f}_n^{(-1)} &= -n^{1/2} \left[ v_d(u) \frac{\partial}{\partial u} + \frac{2\gamma \bar{A}}{v_d(u)} \frac{dU(u)}{du} \right] \\ &\quad - 2n^{3/2} \frac{dv_d(u)}{du}, \end{aligned} \quad (2.28b)$$

$$\hat{f}_n^{(0)} = -n\gamma, \quad (2.28c)$$

$$\hat{f}_n^{(1)} = -(n+1)^{1/2} v_d(u) \frac{\partial}{\partial u} - (n+1)^{3/2} \frac{dv_d(u)}{du}. \quad (2.28d)$$

The hierarchical equation [Eq. (2.27)] is equivalent exactly to the original FPE [Eq. (2.11)]. Multiplicative noise results in the  $u$ -dependent diffusion coefficient and in existence of  $\hat{f}_n^{(-3)} c_{n-3}$  term in Eq. (2.27). The Laplace transform of this type of recurrence equation without the  $\hat{f}_n^{(-3)}$  term was first solved by Brinkman.<sup>22</sup>

### III. ANALYTIC SOLUTIONS OF THE FOKKER-PLANCK EQUATION

#### A. Static distribution functions for the STO

In  $N$ -dimensional ( $N \geq 2$ ) FPE, it is difficult to obtain its stationary solutions because the detailed-balance condition is not satisfied. The relevant FPE [Eq. (2.11)] is written as a continuity equation:

$$\frac{\partial W}{\partial \tau} + \frac{\partial S_u}{\partial u} + \frac{\partial S_{\dot{u}}}{\partial \dot{u}} = 0. \quad (3.1)$$

The  $u$  and  $\dot{u}$  components of the probability current defined as

$$S_u(u, \dot{u}, \tau) \equiv \dot{u} W(u, \dot{u}, \tau), \quad (3.2a)$$

$$\begin{aligned} S_{\dot{u}}(u, \dot{u}, \tau) &\equiv - \left[ \gamma \dot{u} + 2\gamma \bar{A} \frac{dU(u)}{du} \right] W(u, \dot{u}, \tau) \\ &\quad - \gamma v_d^2(u) \frac{\partial W(u, \dot{u}, \tau)}{\partial \dot{u}}, \end{aligned} \quad (3.2b)$$

are generally nonzero in the  $N$ -dimensional FPE system even under the natural boundary condition. Therefore, we shall consider the following case to find a stationary solution analytically. The probability current in  $u$  direction integrated over the velocity  $\dot{u}$  is given by  $c_1(u, \tau)$ , that is,

$$S_u(u, \tau) \equiv \int_{-\infty}^{\infty} S_u(u, \dot{u}, \tau) d\dot{u} = v_d(u) c_1(u, \tau). \quad (3.3)$$

We pay attention in this section to the ‘‘no-current’’ situation where the stationary probability current  $S_u^{\text{st}}(u)$  vanishes, i.e.,  $S_u^{\text{st}}(u) \equiv 0, \forall u$ . This corresponds to the case where the velocity of the Toda oscillator  $\dot{u}$  obeys a Gaussian distribution symmetric around  $\langle \dot{u} \rangle = 0$ , i.e.,

$$\begin{aligned} W^{\text{st}}(u, \dot{u}) &= c_0^{\text{st}}(u) [\Psi_0(\dot{u}; u)]^2 \\ &= \frac{c_0^{\text{st}}(u)}{\sqrt{2\pi v_d(u)}} \exp \left[ -\frac{(\dot{u})^2}{2v_d^2(u)} \right], \end{aligned} \quad (3.4)$$

where the variance of velocity is  $v_d^2(u)$ . This means that the population difference  $\bar{D} = \frac{1}{2}\dot{u} + 1$  also obeys the Gaussian distribution centered at  $\bar{D} = 1$ . This Gaussian character results essentially from the  $S_u^{\text{st}}(u) = 0$  property. In this case, any statistical properties are calculated from only the zeroth coefficient  $c_0^{\text{st}}(u)$ , which must satisfy the equations

$$\hat{f}_1^{(-1)} c_0^{\text{st}}(u) = 0, \quad (3.5a)$$

$$\hat{f}_3^{(-3)} c_0^{\text{st}}(u) = 0. \quad (3.5b)$$

Solving these equations, we obtain an analytic solution of the FPE as a particular solution, which is called the ‘‘no-current’’ (NC) solution hereafter. Other stationary solutions in the case of  $S_u^{\text{st}}(u) \neq 0$  will be discussed in Sec. IV.

#### 1. Negligible field fluctuation ( $S_E = 0$ ) case

Only in this case, the detailed-balance condition and the relation Eq. (3.5b) are automatically satisfied. Then an *exact* stationary solution is easily calculated from the integration of  $\hat{f}_1^{(-1)} c_0^{\text{st}}(u) = 0$  as

$$\begin{aligned} W^{\text{st}}(u, \dot{u}) &= \frac{N}{2\sqrt{S_D}} \exp \left[ -\frac{\gamma \bar{A}}{2S_D} U(u) \right] \\ &\quad \times \exp \left[ -\frac{(\dot{u})^2}{8S_D} \right], \end{aligned} \quad (3.6)$$

where  $N$  is a normalization constant independent of  $u$  and  $\dot{u}$ . As mentioned above, the velocity  $\dot{u}$ , which is connected to the population difference as  $\dot{u} = 2(\bar{D} - 1)$ , obeys the Gaussian distribution corresponding to the Maxwell

distribution of the Brownian particle whose mean velocity is zero and variance of  $\dot{u}$  is  $4S_D$  independent of  $u$ . Although the most probable position  $u^*$  [the position of the local maximum of the distribution function  $W^{\text{st}}(u)$ ] is always zero, which is a potential minimum, the mean value of  $u$  is negative due to the asymmetry of Toda potential which is given as

$$\langle u \rangle = \psi \left[ \frac{\gamma \bar{A}}{2S_D} \right] - \ln \left[ \frac{\gamma \bar{A}}{2S_D} \right], \quad (3.7)$$

where  $\psi(x)$  is the digamma function. This NC solution [Eq. (3.6)] is a well-known distribution function as a ‘‘potential solution.’’

## 2. Weak field fluctuation ( $0 < S_E \ll 4S_D / \bar{A}$ ) case

In this case, the detailed balance is violated so that no potential solution exists. Therefore, no nontrivial NC solution exists in a mathematically rigorous sense because  $\hat{f}_3^{(-3)} c_0^{\text{st}}(u) = 0$  leads to  $c_0^{\text{st}}(u) \equiv 0$ . Even in such a case, FPE can be solved exactly by the aid of MCF, as will be shown in Sec. IV. Before the MCF solutions are discussed, we derive here an approximate but useful solution in this particular case, which is given from integration of Eq. (3.5) as

$$\begin{aligned} W^{\text{st}}(u, \dot{u}) &\simeq \frac{N'}{v_d(u)} \exp \left[ \frac{\gamma \bar{A}}{2S_D} u \right] \\ &\times \left[ 1 + \frac{\bar{A}S_E}{4S_D} e^u \right]^{-(1+2\gamma/S_E + \gamma \bar{A}/2S_D)} \\ &\times \exp \left[ \frac{-(\dot{u})^2}{2v_d^2(u)} \right], \end{aligned} \quad (3.8)$$

with a normalization constant  $N'$ . This result is valid only in the case where the field fluctuation is rather weak in comparison with the population fluctuation, i.e.,  $0 \leq S_E \ll 4S_D / \bar{A}$ . When  $S_E = 0$ , Eq. (3.8) coincides with Eq. (3.6). Similar to the case of  $S_E = 0$ , the velocity distribution is Gaussian symmetric with respect to  $\dot{u} = 0$  with  $u$ -dependent variance of the velocity. The validity of this approximate solution will be confirmed by comparing with the general MCF solution in Sec. IV. The distribution function of  $u$  is derived by integrating  $W^{\text{st}}(u, \dot{u})$  with respect to  $\dot{u}$  as

$$\begin{aligned} W^{\text{st}}(u) &\equiv \int_{-\infty}^{\infty} W^{\text{st}}(u, \dot{u}) d\dot{u} \\ &\simeq N'' \exp \left[ \frac{\gamma \bar{A}}{2S_D} u \right] \\ &\times \left[ 1 + \frac{\bar{A}S_E}{4S_D} e^u \right]^{-(1+2\gamma/S_E + \gamma \bar{A}/2S_D)}. \end{aligned} \quad (3.9)$$

This is illustrated in Fig. 1 for several noise strengths. The distributions are asymmetric and their tails in the  $u < 0$  side are longer than that in the  $u > 0$  side. The most probable positions (the maxima of the distributions)

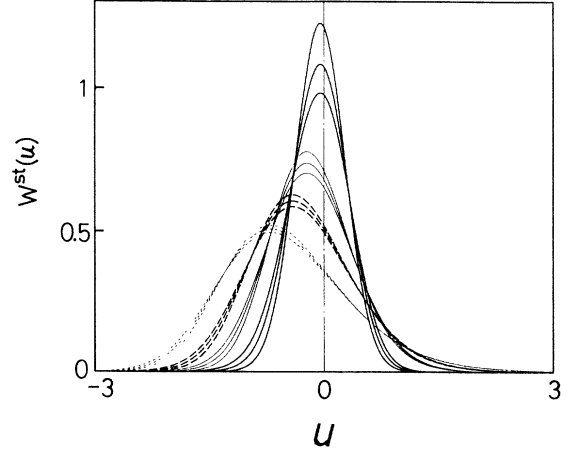


FIG. 1. Probability distribution functions of the STO in the stationary state at  $\bar{A} = 5.0$ . Thick solid lines,  $S_E/\gamma = 0.1$ ; thin solid lines,  $S_E/\gamma = 0.5$ ; thick dashed lines,  $S_E/\gamma = 1.0$ ; and thin dotted lines,  $S_E/\gamma = 1.5$ , with three cases of  $S_D/\gamma = 0.2, 0.3$ , and  $0.4$ . In the cases of large  $S_E/\gamma$ , approximation becomes worse, but the figures are plotted for comparison.

$u^*$  shift from the potential minimum,  $u = 0$ , contrary to the  $S_E = 0$  case [see Eq. (3.6)].

## B. Statistical properties of the light intensity

The normalized intensity of laser radiation is defined as  $\bar{I} = \bar{A}e^u$ , which is normalized to be  $\bar{A}$  in the dynamical (noiseless) case, while the normalized population difference is given as  $\bar{D} = \frac{1}{2}\dot{u} + 1$ . The stationary distribution for the normalized intensity and population difference is derived from  $W^{\text{st}}(u, \dot{u})$  by the relation

$$\begin{aligned} W^{\text{st}}(\bar{I}, \bar{D}) &= \frac{2}{\bar{I}} W^{\text{st}} \left[ \ln \frac{\bar{I}}{\bar{A}}, 2(\bar{D} - 1) \right] \\ &= \left[ \frac{2}{\pi} \right]^{1/2} (S_E \bar{I} + 4S_D)^{-1/2} \\ &\times \exp \left[ -\frac{2(\bar{D} - 1)^2}{S_E \bar{I} + 4S_D} \right] W^{\text{st}}(\bar{I}), \end{aligned} \quad (3.10)$$

where  $W^{\text{st}}(\bar{I})$  is the intensity distribution which is connected to the first expansion coefficient  $c_0^{\text{st}}(u)$  and the probability distribution  $W^{\text{st}}(u, \dot{u})$ , i.e.,

$$\begin{aligned} W^{\text{st}}(\bar{I}) &= \frac{1}{\bar{I}} c_0^{\text{st}} \left[ \ln \frac{2\bar{I}}{\bar{A}} \right] \\ &= \frac{1}{\bar{I}} \int_{-\infty}^{\infty} W^{\text{st}} \left[ \ln \frac{2\bar{I}}{\bar{A}}, \dot{u} \right] d\dot{u}. \end{aligned} \quad (3.11)$$

Using Eq. (3.6), (3.8), or (3.9), we obtain explicit forms of the intensity distribution.

### 1. Negligible field fluctuation ( $S_E = 0$ ) case

In this case, the intensity obeys the  $\Gamma$  distribution with an exponential tail, i.e.,

$$W^{st}(\bar{I}) = \mathcal{N}_1 \bar{I}^{\gamma \bar{A}/2S_D - 1} \exp\left[-\frac{\gamma \bar{I}}{2S_D}\right], \quad (3.12)$$

for  $S_E = 0$ , where  $\mathcal{N}_1$  is the normalization constant:

$$\mathcal{N}_1 = \left[ \frac{\gamma}{2S_D} \right]^{\gamma \bar{A}/2S_D} \left[ \Gamma\left(\frac{\gamma \bar{A}}{2S_D}\right) \right]^{-1}, \quad (3.13)$$

with the gamma function  $\Gamma(x)$ . Equation (3.12) is an exact solution of the FPE. Figure 2 shows the exact intensity distribution [Eq. (3.12)] for several noise strengths. As increasing  $S_D/\gamma$ , maxima of the distribution move to lower intensity, but the tails become longer. The stationary intensity moments exist for an arbitrary order and are of the form

$$\langle \bar{I}^n \rangle = \left[ \frac{2S_D}{\gamma} \right]^n \frac{\Gamma(\gamma \bar{A}/2S_D + n)}{\Gamma(\gamma \bar{A}/2S_D)}, \quad n = 1, 2, \dots \quad (3.14)$$

## 2. Weak field fluctuation ( $0 < S_E \ll 4S_D/\bar{A}$ ) case

While in the case of  $0 < S_E \ll 4S_D/\bar{A}$ , the intensity  $\bar{I}$  and the population difference  $\bar{D}$  have a distribution such as

$$W^{st}(\bar{I}, \bar{D}) \simeq \mathcal{N}_{21} \bar{I}^{\gamma \bar{A}/2S_D - 1} \times \left[ 1 + \frac{S_E \bar{I}}{4S_D} \right]^{-(3/2 + 2\gamma/S_E + \gamma \bar{A}/2S_D)} \times \exp\left[-\frac{2(\bar{D} - 1)^2}{S_E \bar{I} + 4S_D}\right], \quad (3.15)$$

for  $0 < S_E \ll 4S_D/\bar{A}$ . This distribution is symmetric Gaussian for  $\bar{D}$  around  $\langle \bar{D} \rangle = 1$ , but is asymmetric for the intensity  $\bar{I}$ , as shown in Fig. 3. The intensity distri-

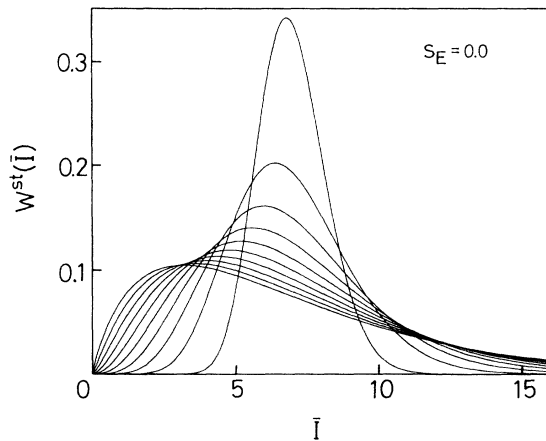


FIG. 2. Exact distribution functions of the normalized intensity of laser light in the stationary state at  $\bar{A} = 7.0$  in the case where field fluctuation is negligible ( $S_E = 0$ ) and  $S_D/\gamma = 0.1, 0.3, \dots, 1.9$ . Increasing  $S_D$ , tails become longer, although  $\langle \bar{I} \rangle$  is always  $\langle \bar{I} \rangle = \bar{A} = 7$ .

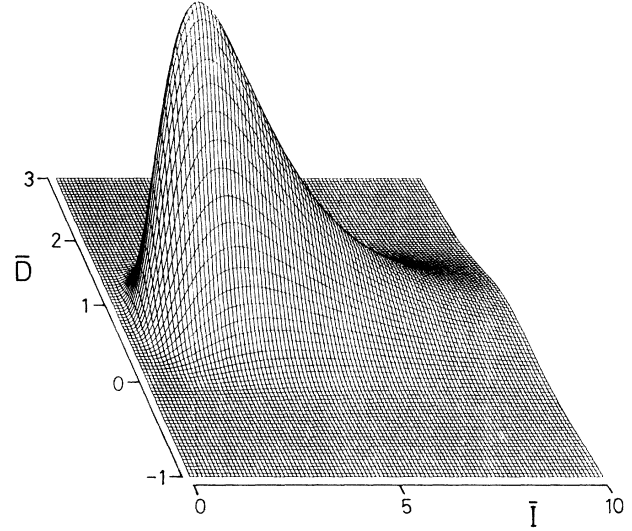


FIG. 3. Three-dimensional plot of the distribution function in  $(\bar{I}, \bar{D})$  space. Parameters are  $\bar{A} = 5.0$ ,  $S_D/\gamma = 0.4$ , and  $S_E/\gamma = 0.5$ .

bution function is of the form

$$W^{st}(\bar{I}) \simeq \mathcal{N}_{22} \bar{I}^{\gamma \bar{A}/2S_D - 1} \times \left[ 1 + \frac{S_E \bar{I}}{4S_D} \right]^{-(1 + 2\gamma/S_E + \gamma \bar{A}/2S_D)}, \quad (3.16)$$

for  $0 < S_E \ll 4S_D/\bar{A}$ , where

$$\mathcal{N}_{22} = \left[ \frac{S_E}{4S_D} \right]^{\gamma \bar{A}/2S_D} \left[ B\left(\frac{\gamma \bar{A}}{2S_D}, 1 + \frac{2\gamma}{S_E}\right) \right]^{-1}, \quad (3.17)$$

and the beta function  $B(x, y)$ . This is similar to the  $F$  distribution. Figure 4 illustrates the intensity distribution

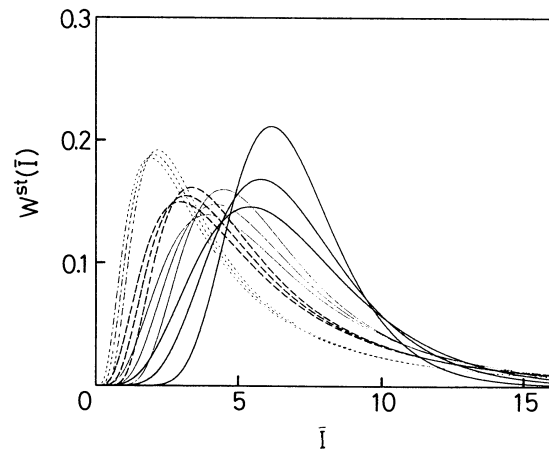


FIG. 4. Approximate distribution functions of the normalized intensity of laser light in the stationary state at  $\bar{A} = 7.0$ . The tails show power decays. Thick solid lines,  $S_E/\gamma = 0.09$ ; thin solid lines,  $S_E/\gamma = 0.5$ ; thick dashed lines,  $S_E/\gamma = 1.0$ ; and thin dotted lines,  $S_E/\gamma = 1.5$ , with three cases of  $S_D/\gamma = 0.15, 0.35$  and  $0.55$ . In the cases of large  $S_E/\gamma$ , approximation becomes worse, but the figures are plotted for comparison.

for several parameters. Contrary to the  $S_E=0$  case, a remarkable feature is the fact that the intensity distribution function [Eq. (3.16)] has a *power tail*, not an exponential one. The exponent of the power tail is evaluated as  $2+2\gamma/S_E$ . This implies a very large fluctuation of the intensity in the bad cavity with field noises. Therefore, the static intensity moments  $\langle \bar{I}^n \rangle$  exist only for integers  $0 < n < 1+2\gamma/S_E$  as

$$\langle \bar{I}^n \rangle = \left[ \frac{4S_D}{S_E} \right]^n B \left[ \frac{\gamma \bar{A}}{2S_D} + n, 1 + \frac{2\gamma}{S_E} - n \right] \times \left[ B \left[ \frac{\gamma \bar{A}}{2S_D}, 1 + \frac{2\gamma}{S_E} \right] \right]^{-1}. \quad (3.18)$$

Only the mean intensity  $\langle \bar{I} \rangle$  always exists regardless of the strength of the field fluctuation to become  $\langle \bar{I} \rangle = \bar{A}$ , which means no shift from the deterministic value in contrast with the good-cavity case in Ref. 3. A novel characteristic is the fact that the  $n$ th intensity moment ( $n \geq 2$ ) diverges as  $S_E/\gamma$  approaches  $2/(n-1)$ . The  $n$ th-order intensity cumulants  $K_n$  are plotted in Fig. 5 showing diverging behaviors, which are defined as

$$\begin{aligned} K_2 &= \langle \bar{I}^2 \rangle - \langle \bar{I} \rangle^2, \\ K_3 &= \langle \bar{I}^3 \rangle - 3\langle \bar{I} \rangle \langle \bar{I}^2 \rangle + 2\langle \bar{I} \rangle^3, \\ K_4 &= \langle \bar{I}^4 \rangle - 3\langle \bar{I}^2 \rangle^2 - 4\langle \bar{I} \rangle \langle \bar{I}^3 \rangle \\ &\quad + 12\langle \bar{I} \rangle^2 \langle \bar{I}^2 \rangle - 6\langle \bar{I} \rangle^4. \end{aligned}$$

The most probable intensity  $\bar{I}^*$  does not coincide with the mean intensity  $\langle \bar{I} \rangle = \bar{A}$ , but

$$\bar{I}^* = \frac{\bar{A} - 2S_D/\gamma}{1 + S_E/\gamma} \leq \bar{A} = \langle \bar{I} \rangle, \quad (3.19)$$

which shows that a peak of  $W^{\text{st}}(\bar{I})$  shifts from  $\langle \bar{I} \rangle$  to a

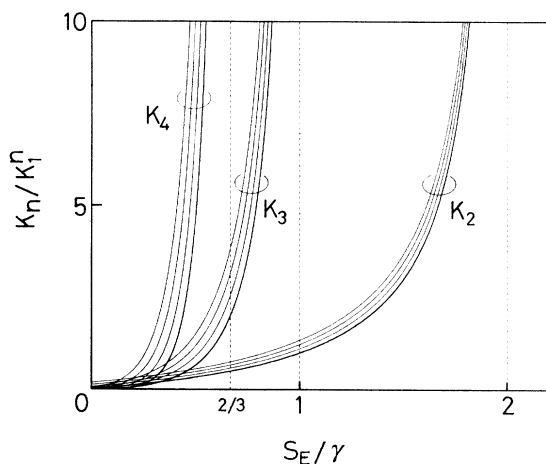


FIG. 5. Stationary cumulants of the intensity normalized by  $K_n^0 = \langle \bar{I} \rangle^n = \bar{A}^n$ . The second-, third-, and fourth-order cumulants in the  $\bar{A}=7.0$  case are plotted as a function of the field noise strength  $S_E/\gamma$  with a parameter  $S_D/\gamma=0.0, 0.2, 0.4$ , and  $0.6$ . Thick lines correspond to the  $S_D=0.0$  case. The second cumulant  $K_2$  is the intensity variance  $\langle (\Delta \bar{I})^2 \rangle$ .

lower value as the noise strengths are increased (see Fig. 4). The skewness  $\alpha_3$  and the flatness  $\alpha_4$  of the intensity distribution are given in our system as  $\alpha_3=2\sqrt{2}S_D/\gamma\bar{A} > 0$  and  $\alpha_4=3+12S_D/\gamma\bar{A} > 3$ , respectively.

In this way, the intensity distribution  $W^{\text{st}}(\bar{I})$  shows explicit differences from the exponential distribution  $(1/\bar{A})\exp(-\bar{I}/\bar{A})$ , which stems from the complex Gaussian statistics<sup>14</sup> of  $\bar{E}$ , where the intensity moments are given as  $\langle \bar{I}^n \rangle = n! \bar{A}^n$ , and the skewness and the flatness are  $\alpha_3=2$  and  $\alpha_4=3+6$ . These are also clearly different from the low- $Q$  cavity case. Therefore, we should not treat the intensity fluctuation in a low- $Q$  cavity as a Gaussian random process.

Last, we refer to the low-intensity limit of the intensity distribution function. In both the cases of  $S_E=0$  and  $0 < S_E \ll 4S_D/\bar{A}$ , the distribution function behaves in the low-intensity limit ( $\bar{I} \ll 1$ ) as

$$\lim_{\bar{I} \rightarrow 0} W^{\text{st}}(\bar{I}) \propto \bar{I}^{\gamma \bar{A}/2S_D - 1}. \quad (3.20)$$

Therefore, the values of the distribution function near  $\bar{I} \sim 0$  vary drastically depending on the ratio  $\gamma \bar{A}/2S_D$ , which are given as zero for  $\gamma \bar{A} > 2S_D$ , a finite value for  $\gamma \bar{A} = 2S_D$ , and  $\infty$  for  $\gamma \bar{A} < 2S_D$ .

### C. Intensity variance and photoelectron statistics

The stationary intensity variance (the second cumulant)  $K_2$  is a good measure of the statistics in order to clarify differences from that in the good-cavity case. The dependence of  $K_2$  on the pump parameter  $\bar{A}$  is one of the most striking features of the intensity statistics in a low- $Q$  cavity. The intensity variance is given from Eq. (3.18) only in the region of  $0 \leq S_E/\gamma < 2$  as

$$\begin{aligned} K_2 &= \langle (\Delta \bar{I})^2 \rangle = \langle \bar{I}^2 \rangle - \langle \bar{I} \rangle^2 \\ &= \frac{S_E/2\gamma}{1 - S_E/2\gamma} \bar{A}^2 + \frac{2S_D/\gamma}{1 - S_E/2\gamma} \bar{A}. \end{aligned} \quad (3.21)$$

This grows in proportion to  $\bar{A}^2$  in the  $S_E \neq 0$  case and in the strong pump limit ( $\bar{A} \gg 1$ ). Other analytical and numerical analyses<sup>6,7</sup> of the Langevin and FPE's of the bad-cavity laser also show the *superlinear* dependence of  $K_2$  upon  $\bar{A}$ , i.e.,  $K_2 \propto \bar{A}^{1+\epsilon}$ , with  $0 \leq \epsilon \leq 1$ . This is clearly different from the good-cavity case<sup>2,3</sup> where the variance is constant, independent of  $\bar{A}$ , or depends linearly or sublinearly on  $\bar{A}$ , i.e.,  $K_2 \propto \bar{A}^{1-\epsilon}$ .

In experiments, the statistical properties of light are usually characterized by the photoelectron counting. The relative deviation from the well-known Poisson statistics (in the case of coherent light) is measured by the photon-number variance,  $\langle (\Delta n)^2 \rangle \equiv \langle (n - \langle n \rangle)^2 \rangle = \langle n \rangle + \eta \langle n \rangle^2$ , where  $n$  is the number of photoelectrons registered in an observation time and  $\eta$  is a photon-counting coefficient which is connected to the intensity moments as<sup>23</sup>

$$\begin{aligned}
\eta &\equiv \frac{\langle (\Delta n)^2 \rangle}{\langle n \rangle^2} - \frac{1}{\langle n \rangle} \\
&= \frac{\langle \bar{I}^2 \rangle}{\langle \bar{I} \rangle^2} - 1 \\
&= \frac{S_E/2\gamma}{1-S_E/2\gamma} + \frac{2S_D/\gamma}{1-S_E/2\gamma} \frac{1}{\bar{A}}, \quad (3.22)
\end{aligned}$$

for  $0 \leq S_E/\gamma < 2$ . This is always positive because we confine our discussion to the classical nature of photons. If we assume that the electric field obeys the complex Gaussian process,  $\eta$  is given as unity, indicating the Bose-Einstein statistics. Contrary to the good-cavity case,<sup>3,4</sup>  $\eta$  tends to a nonzero value as increasing  $\bar{A}$ , as shown in Fig. 6. The first term of the right-hand side of Eq. (3.22) is a measure of the deviation from the Poisson statistics in which  $\eta$  becomes zero. This indicates that the wave property of light remains and shows super-Poisson statistics, in contrast with the coherent emission in the good-cavity laser operating far above threshold where particle picture of light (photon) becomes very good.

In order to make the difference from Poisson statistics clearer, we shall consider the stationary photoelectron counting probability<sup>2</sup>  $P(n, T_{\text{obs}})$  in which  $n$  photoelectrons are registered in an observation time  $T_{\text{obs}}$ . Because quantum effects of photons are neglected, sub-Poissonian character cannot be traced here. We confine ourselves to the case of the short observation time,<sup>24</sup>  $T_{\text{obs}} \ll \tau_c$ , where  $\tau_c$  is an intensity correlation time of the order  $K^{-1}$ . Then, according to Mandel,<sup>25</sup>  $P(n, T_{\text{obs}})$  is given for  $n=0, 1, 2, \dots$  by

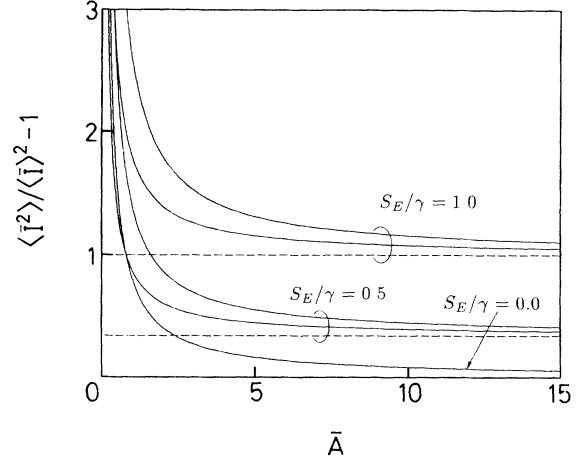


FIG. 6. Photon-counting coefficient  $\eta$  as a function of the pump parameter in the cases of  $S_E/\gamma=0.0, 0.5$ , and  $1.0$ ;  $S_D/\gamma=0.0, 0.2$ , and  $0.4$ . Broken lines are in the  $S_D=0$  case. For the nonzero  $S_E/\gamma$ ,  $\eta$  becomes nonzero even in the strong pump regime. In the region of small  $\bar{A}$  where the STO model is invalid,  $\eta$  diverges.

$$P(n, T_{\text{obs}}) = \frac{1}{n!} \int_0^\infty \xi^n e^{-\xi} W^{\text{st}}(\xi) d\xi, \quad (3.23)$$

$$\xi = \epsilon \int_t^{t+T_{\text{obs}}} \bar{I}(t') dt' \simeq \epsilon T_{\text{obs}} \bar{I}, \quad (3.24)$$

where  $W^{\text{st}}(\xi)$  is the stationary intensity distribution and  $\epsilon$  is an efficiency of the detector.

An integral form of  $P(n, T_{\text{obs}})$  for  $0 < S_E \ll 4S_D/\bar{A}$  is given by Eqs. (3.16) and (3.23) as

$$P(n, T_{\text{obs}}) = \frac{\mathcal{N}}{n! (\epsilon T_{\text{obs}})^{\gamma \bar{A}/2S_D}} \int_0^\infty \xi^{n+\gamma \bar{A}/2S_D-1} e^{-\xi} \left[ 1 + \frac{S_E \xi}{4S_D \epsilon T_{\text{obs}}} \right]^{-(1+2\gamma/S_E + \gamma \bar{A}/2S_D)} d\xi, \quad (3.25)$$

where the photoelectron variance is *always* larger than the average number of photocounts  $\langle n \rangle$  (super-Poissonian).

Explicit expression is obtained only in the  $S_E=0$  case to show the *negative binomial* distribution for  $n=0, 1, 2, \dots$ , i.e.,

$$P(n, T_{\text{obs}}) = \frac{1}{n!} \frac{\Gamma(n + \gamma \bar{A}/2S_D)}{\Gamma(\gamma \bar{A}/2S_D)} \left[ \frac{\gamma}{2S_D \epsilon T_{\text{obs}}} \right]^{\gamma \bar{A}/2S_D} \left[ 1 + \frac{\gamma}{2S_D \epsilon T_{\text{obs}}} \right]^{-(n + \gamma \bar{A}/2S_D)}. \quad (3.26)$$

Here the average number of photocounts is given as  $\langle n \rangle = \epsilon T_{\text{obs}} \bar{I}$ , and the photoelectron variance is larger than  $\langle n \rangle$  (super-Poissonian), i.e.,  $\langle (\Delta n)^2 \rangle = \langle n \rangle (1 + 2\epsilon T_{\text{obs}} S_D/\gamma) > \langle n \rangle$ . In addition, the skewness  $\alpha_3$  and flatness  $\alpha_4$  of the photoelectron distribution are evaluated as

$$\alpha_3 = \frac{1 + 4\epsilon T_{\text{obs}} S_D/\gamma}{[\epsilon T_{\text{obs}} \bar{A} (1 + 2\epsilon T_{\text{obs}} S_D/\gamma)]^{1/2}} > \alpha_3^P > 0, \quad (3.27a)$$

$$\alpha_4 = 3 + \frac{1 + 12\epsilon T_{\text{obs}} S_D/\gamma + 24\epsilon^2 T_{\text{obs}}^2 S_D^2/\gamma^2}{\epsilon T_{\text{obs}} \bar{A} (1 + 2\epsilon T_{\text{obs}} S_D/\gamma)} > \alpha_4^P > 3, \quad (3.27b)$$

where  $\alpha_3^p$  and  $\alpha_4^p$  are those of the Poisson distribution approximating Eq. (3.26), i.e.,  $\alpha_3^p = (\epsilon T_{\text{obs}} \bar{A})^{-1/2}$  and  $\alpha_4^p = 3 + (\epsilon T_{\text{obs}} \bar{A})^{-1}$ . This shows that the negative binomial distribution has a longer tail than that of the Poisson distribution. In an artificial limit of  $\bar{A} \rightarrow \infty$  with  $\langle n \rangle$  constant, this approaches the Poisson distribution  $\langle n \rangle^n e^{-\langle n \rangle} / n!$ . It should be noted in addition that the Poisson distribution appears also in the limit of  $S_D \rightarrow 0$  with a fixed  $\bar{A}$ . This limit corresponds to the coherent light case without noises. On the other hand, Eq. (3.25) for the  $S_E > 0$  case does not approach the Poisson distribution in any limits, which differs also from the Bose-Einstein distribution or the negative binomial distribution. Anyway, both the distribution functions [Eqs. (3.25) and (3.26)] are characterized by their longer tails than that of the Poisson distribution. Thus laser emission in the bad cavity yields a novel super-Poissonian photoelectron statistics regardless of the field noise strength  $S_E$ .

Here we shall compare this STO model with the phenomenological Langevin force model employed in our previous paper<sup>6</sup> to clarify differences in results obtained by above two methods. The principal differences are as follows. The STO model is useful only when (i) the atomic polarization noise is negligible and (ii) the pumping is relatively strong. On the other hand, the latter Langevin method is free of the above limitations; that is, it is valid for an arbitrary pumping rate and arbitrary noise strengths (including polarization noise). More general discussion on the statistical properties can be done by the latter method. However, it does not lead to analytical solutions of the Fokker-Planck equation; therefore, we cannot help doing numerical calculations in the latter analysis. In spite of the above constraints, on the other hand, analytical discussion is possible by the STO method. It is difficult to trace power tail characteristics by numerical approaches in the latter model, and they should be clarified analytically in the STO method. Here we note that a singularity of the intensity distribution function near  $\bar{I}=0$  was observed in the latter Langevin model for  $\gamma \bar{A} / 2S_D > 1$  where no singularity is expected

in the STO result (with no polarization noise). This singularity, therefore, may be due to the atomic polarization fluctuation which induces background noise in the light intensity, resulting in a singular peak of  $W^{\text{st}}(\bar{I} \simeq 0)$ . Because two methods are substantially different in terms of the considered situations, it is meaningless to simply compare only the results

#### IV. GENERAL SOLUTIONS IN TERMS OF THE MATRIX CONTINUED FRACTION

In the preceding section, we discuss only the no-current case where the first expansion coefficient  $c_0(u, \tau)$  plays a dominant role. In the case of nonvanishing probability current  $S_u^{\text{st}}(u) \neq 0$ , on the other hand, all expansion coefficients  $c_n^{\text{st}}(u)$  for  $n=0, 1, 2, \dots$  are necessary in discussing the solution of the FPE. This procedure can be carried out in a closed form with the aid of the matrix continued fraction (MCF), whose derivation and procedure are reviewed in the Appendix. Hereafter, we call this general solution calculated by MCF as the ‘‘MCF solution,’’ which is an exact, closed-form, and nonperturbative solution of FPE’s. This general solution is used also for the checking an approximate solution.

A significant difference between the NC solution [in the  $S_u^{\text{st}}(u) \equiv 0$  case] and the MCF solution [in the  $S_u^{\text{st}}(u) \neq 0$  case] is clarified most clearly by comparing the distribution function of the velocity of a Toda oscillator  $W^{\text{st}}(\dot{u})$  with the Gaussian distribution. The velocity distribution function for the STO under the no-current condition is given from Eq. (3.4) as a Gaussian:

$$W_{\text{NC}}^{\text{st}}(\dot{u}) = \frac{1}{v_d \sqrt{2\pi}} \exp \left[ -\frac{(\dot{u})^2}{2v_d^2} \right], \quad (4.1)$$

whose mean velocity is zero, i.e.,  $\langle \dot{u} \rangle = 0$ , and the velocity variance is given by  $v_d^2$ . Unfortunately, no analytical expression of  $W_{\text{NC}}^{\text{st}}(\dot{u})$  is obtained in the case of  $0 < S_E \ll 4S_D / \bar{A}$ . The corresponding velocity distribution of the MCF solution is

$$W_{\text{MCF}}^{\text{st}}(\dot{u}) = W_{\text{NC}}^{\text{st}}(\dot{u}) + \frac{1}{\sqrt{2\pi}} \sum_{n=1}^{\infty} \frac{a_n^0}{\sqrt{n!}} \exp \left[ -\frac{(\dot{u})^2}{2v_d^2} \right] H_n \left[ \frac{\dot{u}}{v_d} \right] \frac{1}{v_d}, \quad (4.2)$$

whose mean velocity is  $\langle \dot{u} \rangle = v_d a_1^0$  and the velocity variance is  $v_d^2 [1 - (a_1^0)^2 + a_2^0]$ . Here  $a_n^0$  ( $n=1, 2, \dots$ ) are the expansion coefficients in the MCF. Numerical calculation is carried out in the case of  $0 < S_E \ll 4S_D / \bar{A}$  to compare the velocity distributions of the NC and MCF solutions. Figure 7 shows two velocity distributions which are calculated from Eqs. (3.8) and (4.2). The difference between them is small, and the MCF solution is similar to the Gaussian, although the mean velocity becomes slightly positive ( $a_1^0 > 0$ ) due to the anticorrelation between  $u$  and  $\dot{u}$ .

Here we point out that there is also little difference be-

tween the position distribution functions  $W_{\text{NC}}^{\text{st}}(u)$  and  $W_{\text{MCF}}^{\text{st}}(u)$  in both cases of  $S_E = 0$  and  $0 < S_E \ll 4S_D / \bar{A}$ . Therefore, the NC approximate solutions [Eqs. (3.8) and (3.9)] are valid and useful enough unless the noise strength  $S_E$  is so large. As a result, the intensity distributions in both the cases of  $S_u^{\text{st}}(u) = 0$  and  $\neq 0$ , i.e.,  $W_{\text{NC}}^{\text{st}}(\bar{I})$  and  $W_{\text{MCF}}^{\text{st}}(\bar{I})$  are almost identical in the physical region of the parameters within a numerical error, particularly in the low-friction limit ( $\gamma = \gamma_{\parallel} / \gamma_{\perp}$  is small). This has been confirmed also by an analysis of the Brownian motion in a periodic potential.<sup>17</sup> Because no remarkable difference between them is found, we conclude that

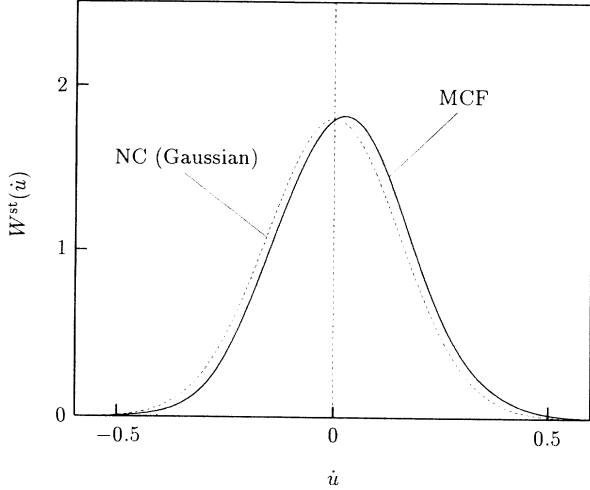


FIG. 7. Velocity distribution function of the STO. The thick line is obtained by the numerical MCF calculation [Eq. (4.2)]; the thin dotted line is Gaussian given by the analytical NC solutions [Eq. (3.8)]. Parameters are  $\bar{A}=5.0$ ,  $S_D/\gamma=0.06$ , and  $S_E/\gamma=0.2$ .

analytical (exact and approximate) expressions of the stationary solution under the no-current condition are of validity.

## V. COMPARISON WITH THE GOOD-CAVITY CASE

### A. Modified stochastic Toda-oscillator equation

Comparing with the bad-cavity case, we present the results of the STO analysis for the good-cavity case ( $\gamma_\perp > K, \gamma_\parallel$ ) to root out differences between them. Under the good-cavity condition, the polarization can be adiabatically eliminated from the Langevin Maxwell-Bloch equations [Eq. (2.1)]. A similar procedure to the bad-cavity case leads to the Langevin equation in the good-cavity case:

$$\begin{aligned} \frac{d^2 u}{d\tau^2} + \gamma(1 + \bar{A}e^u) \frac{du}{d\tau} + 2\kappa\gamma \bar{A} \frac{dU(u)}{du} \\ = 2\kappa(\gamma S_D)^{1/2} \Gamma_3(\tau) \\ + \kappa(\gamma \bar{A} S_P)^{1/2} e^{u/2} \sin\theta \Gamma_3(\tau) \\ - \kappa(\gamma \bar{A} S_P)^{1/2} e^{u/2} \cos\theta \Gamma_4(\tau), \end{aligned} \quad (5.1)$$

where  $u(\tau) \equiv 2 \ln |\bar{E}(\tau)|$ ,  $\kappa \equiv K/\gamma_\perp$  is a scaled field decay rate,  $\theta \equiv \arg E$  is the phase of the total field which is nearly constant, and  $U(u)$  is the Toda potential. The field noise is suppressed under a relatively high pumping, contrary to the bad-cavity case where the field and population fluctuations become dominant in the strong pump regime. Therefore,  $S_P$  and  $S_D$  terms play essential roles in the good-cavity stochastic system. This is the modified STO equation. An important difference lies in a friction term of the Toda oscillator. In contrast to the bad-cavity case, the *position-dependent* friction appears, in addition to the position-dependent fluctuations, to show a very strong dissipation in the large  $u$  region. This results from

the nonlinear coupling between the population of material and the electric field in the Maxwell-Block equations of the good-cavity case, as shown later.

The Fokker-Planck operator is then given as

$$\begin{aligned} \mathcal{L}_{\text{FP}}^{\text{good}}(u, \dot{u}) = -\dot{u} \frac{\partial}{\partial u} + 2\kappa\gamma \bar{A} \left[ \frac{dU(u)}{du} \right] \frac{\partial}{\partial \dot{u}} \\ + \gamma \frac{\partial}{\partial \dot{u}} \left[ (1 + \bar{A}e^u) \dot{u} + \kappa^2 v_p^2(u) \frac{\partial}{\partial \dot{u}} \right], \end{aligned} \quad (5.2)$$

where the  $u$ -dependent diffusion coefficient is  $\gamma\kappa^2 v_p^2(u)$  with the  $u$ -dependent diffusion velocity  $v_p(u) = (S_P \bar{A} e^u + 4S_D)^{1/2}$ . The probability distribution is expanded by the complete orthogonal set as

$$W_{\text{good}}(u, \dot{u}, \tau) = \Phi_0(\dot{u}; u) \sum_{n=0}^{\infty} d_n(u, \tau) \Phi_n(\dot{u}; u), \quad (5.3a)$$

$$\begin{aligned} \Phi_n(\dot{u}, u) = \frac{1}{[n! \sqrt{2\pi} v_{\text{eff}}(u)]^{1/2}} \exp \left[ -\frac{(\dot{u})^2}{4v_{\text{eff}}^2(u)} \right] \\ \times H_n \left[ \frac{\dot{u}}{v_{\text{eff}}(u)} \right]. \end{aligned} \quad (5.3b)$$

Here  $v_{\text{eff}}(u)$  is an effective diffusion velocity, defined as

$$\begin{aligned} v_{\text{eff}}(u) &\equiv \frac{\kappa v_p(u)}{(1 + \bar{A}e^u)^{1/2}} \\ &= \kappa \left[ \frac{S_P \bar{A} e^u + 4S_D}{\bar{A}e^u + 1} \right]^{1/2}. \end{aligned} \quad (5.4)$$

Even in the additive noise only ( $S_P=0$ ), the effective diffusion depends on the position variable.

The one-sided recurrence equation of motion for the expansion coefficients  $d_n(u, \tau)$ ,  $n=0, 1, 2, \dots$ , is given by the use of orthonormal property of  $\Phi_n$  as

$$\begin{aligned} \frac{\partial d_n(u, \tau)}{\partial \tau} = \hat{g}_n^{(-3)} d_{n-3} + \hat{g}_n^{(-1)} d_{n-1} \\ + \hat{g}_n^{(0)} d_n + \hat{g}_n^{(1)} d_{n+1}, \end{aligned} \quad (5.5)$$

where  $d_n(u, \tau) = 0$  for  $n < 0$  and  $\hat{g}_n^{(k)}$  are the expansion-coefficient operators with respect to  $u$  given as

$$\hat{g}_n^{(-3)} = -[n(n-1)(n-2)]^{1/2} \frac{dv_{\text{eff}}(u)}{du}, \quad (5.6a)$$

$$\begin{aligned} \hat{g}_n^{(-1)} = -n^{1/2} \left[ v_{\text{eff}}(u) \frac{\partial}{\partial u} + \frac{2\kappa\gamma \bar{A}}{v_{\text{eff}}(u)} \frac{dU(u)}{du} \right] \\ - 2n^{3/2} \frac{dv_{\text{eff}}(u)}{du}, \end{aligned} \quad (5.6b)$$

$$\hat{g}_n^{(0)} = -n\gamma(1 + \bar{A}e^u), \quad (5.6c)$$

$$\begin{aligned} \hat{g}_n^{(1)} = -(n+1)^{1/2} v_{\text{eff}}(u) \frac{\partial}{\partial u} \\ - (n+1)^{3/2} \frac{dv_{\text{eff}}(u)}{du}. \end{aligned} \quad (5.6d)$$

### B. Analytic solutions in the no-current case

Under the no-current condition, we get a static probability distribution of  $u$  by integrating  $\hat{g}_1^{(-1)} d_0^{\text{st}}(u) = 0$  as

$$W_{\text{good}}^{\text{st}}(u) = N_g (\bar{A} e^u + 1) [v_p^2(u)]^{2\mu-1} \times \exp \left[ -\frac{\gamma \bar{A}}{2\kappa S_D} \left( \frac{4S_D}{S_P} e^u - u \right) \right], \quad (5.7)$$

where  $N_g$  is a normalization constant and

$$\mu \equiv \frac{\gamma}{\kappa S_P} \left[ \frac{4S_D}{S_P} - 1 \right] \left[ \frac{S_P \bar{A}}{4S_D} + 1 \right]. \quad (5.8)$$

This solution is exact when  $S_P = 4S_D$ , (i.e.,  $\mu = 0$ ). In the case where  $\mu$  is nonzero but small (i.e.,  $|\mu| \sim 0$ ), it is approximate but nearly exact. In the former case ( $\mu = 0$ ), although both the diffusion and friction depend on  $u$ , their  $u$  dependence cancels with each other to lead an exact solution. The case of  $\mu \sim 0$  corresponds to the case of  $2\gamma_{\parallel}(N_2 - N_1) \sim \mathcal{S}_D^{\text{ex}} - 2\gamma \mathcal{S}_P^{\text{exp}} > 0$ . Because  $\gamma$  is very small for ordinary laser material, the situation  $\mu \sim 0$  is realizable if we control the external component of the population noise (pump noise). Next, we shall calculate the intensity distribution functions with the use of Eq. (5.7)

#### 1. $S_P = 4S_D$ ( $\mu = 0$ ) case

In spite of the fact that both the additive and multiplicative noises exist in this case, the effective diffusion velocity does not depend on the position variable  $u$ ; that is, the  $u$ -dependent friction and  $u$ -dependent diffusion are balanced. Then we can obtain an exact solution of the FPE. The stationary intensity distribution in the  $S_P = 4S_D$  case has a similar form to the bad-cavity case ( $\Gamma$  distribution):

$$W_{\text{good}}^{\text{st}}(\bar{I}) = \mathcal{N}_{g1} \bar{I}^{2\nu-1} \exp \left[ -\frac{2\nu \bar{I}}{\bar{A}} \right], \quad (5.9)$$

where

$$\langle \bar{I}^n \rangle = \frac{\Gamma(2\nu+n)}{\Gamma(2\nu)} q^{n/2} [W_{\mu-\nu-n/2, \mu+\nu+n/2-1/2}(p) + (2\nu+n)\sqrt{q} W_{\mu-\nu-n/2-1/2, \mu+\nu+n/2}(p)] \times [W_{\mu-\nu, \mu+\nu-1/2}(p) + 2\nu\sqrt{q} W_{\mu-\nu-1/2, \mu+\nu}(p)]^{-1}. \quad (5.15)$$

In the good-cavity limit ( $\kappa/\gamma \rightarrow 0$ ) or the small  $S_D$  limit (accordingly,  $S_P$  is also small), we find that the mean intensity is given as  $\langle \bar{I} \rangle \simeq S_P \bar{A} / 4S_D$  and the intensity variance is  $\langle (\Delta \bar{I})^2 \rangle \simeq \kappa S_P^2 \bar{A} / 8\gamma S_D$ , showing a linear dependence on  $\bar{A}$ . This is a clear difference from the bad-cavity case.

In the good-cavity case, the intensity distribution has no power tail and the intensity variance is only linearly

$$\mathcal{N}_{g1} = \left[ \frac{2\nu}{\bar{A}} \right]^{2\nu} \frac{1}{\Gamma(2\nu)}, \quad (5.10a)$$

$$\nu = \frac{\gamma \bar{A}}{4\kappa S_D}. \quad (5.10b)$$

The intensity moments are given for  $n = 1, 2, \dots$  as

$$\langle \bar{I}^n \rangle = \frac{\Gamma(2\nu+n)}{\Gamma(2\nu)} \left[ \frac{\bar{A}}{2\nu} \right]^n. \quad (5.11)$$

The mean intensity is  $\langle \bar{I} \rangle = \bar{A}$ , which is the same as that in the bad-cavity case. However, the intensity variance is linearly proportional to the pump parameter, i.e.,  $K_{\text{good}}^{\text{st}} = \langle (\Delta \bar{I})^2 \rangle = 2\kappa S_D \bar{A} / \gamma \propto \bar{A}$ .

#### 2. $S_P \sim 4S_D$ ( $|\mu| \sim 0$ ) case

A remarkable difference of the intensity statistics lies in the fact that no power tail distribution is obtained in any parameter region of the good-cavity case, i.e.,

$$W_{\text{good}}^{\text{st}}(\bar{I}) = \mathcal{N}_{g2} (\bar{I} + 1) (S_P \bar{I} + 4S_D)^{2\mu-1} \times \bar{I}^{2\nu-1} \exp \left[ -\frac{2\nu \bar{I}}{\bar{A}} \right], \quad (5.12)$$

where the normalization constant is given as

$$\mathcal{N}_{g2}^{-1} = \frac{\Gamma(2\nu) S_P}{4S_D} q^{\mu+\nu} e^{p/2} \times [W_{\mu-\nu, \mu+\nu-1/2}(p) + 2\nu\sqrt{q} W_{\mu-\nu-1/2, \mu+\nu}(p)], \quad (5.13)$$

and

$$p = \frac{8\gamma S_D}{\kappa S_P^2}, \quad (5.14a)$$

$$q = \frac{2\kappa S_D}{\gamma}. \quad (5.14b)$$

Here  $W_{\alpha, \beta}(z)$  is Whittaker's function.<sup>26</sup> This distribution function has an exponential tail. Therefore, any order of intensity moments exist for all integers  $n = 1, 2, \dots$  as

proportional to the pump parameter. Thus intensity fluctuation of the good-cavity system is weaker than that of the bad-cavity system, particularly in the strong pump regime. This comes from the gain saturation mechanism of the good-cavity laser where intracavity field becomes intense to induce stronger interaction with the population of the material (multiplicative feedback of the field to the material) in comparison with the bad-cavity case (only

additive feedback resulting from weak field intensity due to a large cavity loss). In the good-cavity case, the gain factor  $G$  is subjected to a *nonlinear saturation*, while the gain factor of the bad-cavity laser suffers only a *linear depletion*, that is

$$G_{\text{good}} = \frac{G_{\text{good}}^0}{1 + \bar{I}/\bar{I}_s}, \quad (5.16a)$$

$$G_{\text{bad}} = G_{\text{bad}}^0 - 2\gamma_1 \bar{I}, \quad (5.16b)$$

where  $G_{\text{good}}^0 = 2K(\bar{A} + 1)$  and  $G_{\text{bad}}^0 = 2\gamma_1(\bar{A} + 1)$  are linear (unsaturated) gains of the good- and bad-cavity systems, respectively, and  $\bar{I}_s = 1$  is a saturation intensity. Therefore, remarkable differences appear in the large intensity region ( $\bar{I} > 1$ ). This induces enhancement of the friction for the modified STO in the large  $u$  region resulting in the suppression of intensity fluctuation in the large  $\bar{I}$  region of the high- $Q$  cavity case.

Last, we refer to the photoelectron counting probability which is evaluated analytically for a short observation time only in the case of  $\mu = 0$  as

$$P(n, T_{\text{obs}}) = \frac{1}{n!} \frac{\Gamma(2\nu + n)}{\Gamma(2\nu)} \left[ \frac{\gamma}{2S_D \epsilon \kappa T_{\text{obs}}} \right]^{2\nu} \times \left[ 1 + \frac{\gamma}{2S_D \epsilon \kappa T_{\text{obs}}} \right]^{-(2\nu + n)}, \quad (5.17)$$

whose mean is the same as that of Eq. (3.26), i.e.,  $\langle n \rangle = \epsilon T_{\text{obs}} \bar{A}$ . The photoelectron variance is different from the bad-cavity case by a factor  $\kappa$ , i.e.,  $\langle (\Delta n)^2 \rangle = \langle n \rangle (1 + 2\epsilon T_{\text{obs}} S_D \kappa / \gamma)$ . Therefore, in the

good-cavity limit ( $\kappa/\gamma \ll 1$ ), the variance becomes  $\langle (\Delta n)^2 \rangle = \langle n \rangle$  to indicate the well-known Poisson statistics where the fluctuation of the light wave is negligible and the discreteness of the photoelectrons plays a dominant role in photon-counting statistics.

## VI. DISCUSSION AND CONCLUSIONS

At first, comparing with NC solutions and MCF ones, we discuss their realizability of the probability distribution in terms of the pseudoenergy of the STO. The pseudoenergy  $\mathcal{E}(u, \dot{u})$  of the STO is defined as

$$\begin{aligned} \mathcal{E}(u, \dot{u}) &\equiv \frac{(\dot{u})^2}{2} + 2\gamma \bar{A} U(u) \\ &= 2(\bar{D} - 1)^2 + 2\gamma \bar{A} \left[ \frac{\bar{I}}{\bar{A}} - \ln \frac{\bar{I}}{\bar{A}} - 1 \right]. \end{aligned} \quad (6.1)$$

The first and second terms of the right-hand side of Eq. (6.1) correspond to the kinetic and potential energy parts, respectively. The distribution function may be given to minimize the mean energy:

$$\langle \mathcal{E} \rangle = \int_{-\infty}^{\infty} d\dot{u} \int_{-\infty}^{\infty} du \mathcal{E}(u, \dot{u}) \mathcal{W}^{\text{st}}(u, \dot{u}). \quad (6.2)$$

Using the NC solution in Sec. III, mean energy is analytically calculated and of the form

$$\langle \mathcal{E} \rangle_{\text{NC}} = 2S_D + 2\gamma \bar{A} \left[ \ln \left[ \frac{\gamma \bar{A}}{2S_D} \right] - \psi \left[ \frac{\gamma \bar{A}}{2S_D} \right] \right] \text{ for } S_E = 0. \quad (6.3)$$

In the strong pump limit ( $\bar{A} \gg 1$ ) or the weak population noise limit ( $S_D/\gamma \ll 1$ ), this approaches  $4S_D$ . In the case of the MCF solution, on the other hand, we have

$$\begin{aligned} \langle \mathcal{E} \rangle_{\text{MCF}} &= 2S_D (1 + \sqrt{2} a_2^0) + 2\gamma \bar{A} \sum_{n=1}^{\infty} \sum_{m=0}^{\infty} \sum_{r=0}^m (-1)^r (2r-1)!! (2n+2m-2r-1)!! \frac{\alpha^{2n}}{(2n)! \sqrt{(2m)!}} \begin{Bmatrix} 2m \\ 2r \end{Bmatrix} \\ &\times \left[ a_0^{2m} + \frac{\alpha a_0^{2m+1}}{(2n+1)\sqrt{2m+1}} \frac{(2n+2m-2r+1)(2m+1)}{2m-2r+1} \right]. \end{aligned} \quad (6.4)$$

According to numerical calculations, there is little or no difference between Eqs. (6.3) and (6.4). Therefore, their realizabilities are almost the same in a parameter region ( $0 \leq S_E \ll 4S_D/\bar{A}$ ). This is another confirmation for the validity and usefulness of the analytic NC solutions.

The temporal stability of the stationary solution should be clarified by solving the eigenvalue problem of the Fokker-Planck operator.<sup>17</sup> The eigenvalue  $\lambda$  of the Fokker-Planck operator satisfies the eigenvalue equation<sup>27</sup> for  $n=0, 1, 2, \dots$ , i.e.,

$$\det[\underline{M}_n^- \tilde{\underline{S}}_{n-1}(\lambda) + \underline{M}_n - \lambda \underline{I} + \underline{M}_n^+ \tilde{\underline{S}}_n(\lambda)] = 0, \quad (6.5)$$

where  $\underline{I}$  is a unit matrix and  $\tilde{\underline{S}}_n(\lambda)$  is a reduced transfer matrix which satisfies the MCF relation [see Eq. (A9)] for  $n=0, 1, 2, \dots$ , i.e.,

$$\tilde{\underline{S}}_n(\lambda) = -[\underline{M}_n - \lambda \underline{I} + \underline{M}_{n+1}^+ \tilde{\underline{S}}_{n+1}(\lambda)]^{-1} \underline{M}_{n+1}^-. \quad (6.6)$$

Here  $\underline{M}_n$  and  $\underline{M}_n^\pm$  are coefficient matrices defined in the Appendix.

We have solved numerically the above eigenvalue equation to obtain the following results. (i) The largest eigenvalue is always zero,  $\lambda_{\text{max}} = 0$ , independent of parameters  $\bar{A}$ ,  $S_E$  and  $S_D$ , and (ii) the other eigenvalues are all negative. This means that the stationary solution of FPE is marginally stable. Therefore, the stationary distribution functions obtained in this paper can exist in a physical sense. Detailed results on the eigenvalue analysis will be reported elsewhere.<sup>28</sup> Anyhow, particular solutions of the FPE (i.e., the NC solutions) almost coincide with the general MCF solutions in the parameter region  $0 \leq S_E \ll 4S_D/\bar{A}$ . Their realizability and stability have been

checked; therefore, analytical solutions are useful enough to discuss the statistical characteristics without the use of more complicated MCF ones.

Finally, we refer to the controllability of noise strengths,  $S_E$  and  $S_D$ , in actual experimental situations. These values are given as

$$S_E = \left[ \frac{2}{gD_{\text{th}}} \right]^2 \left[ \frac{2K}{e^{\hbar\omega_c/k_B T} - 1} + \mathcal{S}_E^{\text{ex}} \right], \quad (6.7a)$$

$$S_D = \frac{\gamma_{\perp}}{2\gamma_{\parallel}} \left[ \frac{1}{\gamma_{\perp} D_{\text{th}}} \right]^2 (2\gamma_{\parallel} N + \mathcal{S}_D^{\text{ex}}). \quad (6.7b)$$

Here  $S_E$  is controlled mainly by the field decay rate  $K$ , which depends on the cavity mirror reflectivity  $R$ , viz.,  $K = \kappa + (c/L)|\ln R|$  (where  $\kappa$  stands for a loss rate in the gain medium resulting from absorption, diffraction, and so on). We consider an additional term  $\mathcal{S}_E^{\text{ex}}$  as an arbitrary injection noise field to vary the field noise strength in this analysis. On the other hand,  $S_D$  is usually fixed when the total number of active atoms (or carriers) is given. However, we vary  $\mathcal{S}_D^{\text{ex}}$  by controlling pumping sources (e.g., injection current supply or pumping light). It is usually difficult to give *a priori* the expected values of these noise strengths because many factors contribute these values. They would rather be determined by the observed statistical properties of light. Typical and reasonable values are employed in the numerical calculations of this paper.

The main results of this paper are summarized below.

(i) The stochastic Toda-oscillator equation is derived for the first time to study the statistical characters of a low- $Q$  cavity laser. It is transformed to the Fokker-Planck equation with a position-dependent diffusion coefficient and is solved exactly or approximately with the aid of the complete orthogonal-function expansion.

(ii) Particular solutions of FPE are analytically obtained under the no-current condition to show a long tail (power tail) of the intensity distribution. Stationary intensity variance is investigated as an example for clarifying novel statistics due to the power tail. Super-Poissonian photoelectron statistics is also examined.

(iii) General solutions are also obtained in a closed form and are calculated numerically with the use of the matrix continued fraction. Using them, the probability distribution of the velocity of Toda oscillator (the population difference) is discussed. Analytical particular solutions are shown to be valid and useful enough in a physical parameter space.

(iv) A modified STO equation in the good-cavity case is derived and investigated to clarify an essential difference between the good- and bad-cavity conditions. In the former case, the position-dependent friction of the Toda oscillator appears and the intensity distribution has no power tail, resulting from the strong gain saturation.

In the next step of this work, we need to pay attention to the spatial coherence and spatial inhomogeneity which may play a crucial role in the low- $Q$  cavity. Then we must give up the uniform-field and plane-wave approximations. Then the problem becomes multidimensional in the space coordinate and hard to solve analytically but

interesting in terms of the spatiotemporal stochastic system and noise-induced pattern formation. Another extension of this work is to construct the quantum-mechanical version of the STO. Interplay between the nonclassical nature of photons and the external fluctuation is still controversial and to be clarified. These problems are left for future studies.

#### ACKNOWLEDGMENTS

The author would like to thank Professor E. Hanamura, Professor J. Satsuma, Dr. N. Nagaosa, Professor R. Ito, Professor F. Shimizu, Dr. M. Kuwata-Gonokami, and Professor H. Risken for helpful discussions and encouragement. He is also grateful to Dr. Y. Yamamoto, Dr. N. Imoto, and M. Ueda for sending him useful comments on the Langevin Maxwell-Bloch equations and the photoelectron statistics. This work was supported in part by the Scientific Grang-in-Aid from the Ministry of Education, Science, and Culture of Japan.

#### APPENDIX: THE MATRIX CONTINUED-FRACTION SOLUTION

In the case of nonvanishing probability current, we need to consider all expansion coefficients  $c_n(u, \tau)$  for  $n=0, 1, 2, \dots$ . This procedure can be carried out with the aid of the matrix continued fraction according to Risken.<sup>17</sup> In the first step, we further expand  $c_n(u, \tau)$  into the complete set with respect to  $u$  to satisfy its boundary condition [Eq. (2.20)] as

$$c_n(u, \tau) = \frac{1}{\alpha\sqrt{2\pi}} \sum_{p=0}^{\infty} \frac{a_n^p(\tau)}{\sqrt{p!}} \exp\left[-\frac{u^2}{2\alpha^2}\right] \times H_p\left[\frac{u}{\alpha}\right], \quad (A1)$$

where  $a_n^p(\tau)$  is an expansion coefficient ( $a_n^p=0$  for  $n, p < 0$ ) and the factor  $\alpha > 0$  is an arbitrary scaling parameter which is introduced in order to improve the convergence of the expansion in the numerical calculation. In this procedure, the exponential terms in the potential and diffusion coefficient are also expanded to a power series, and integrations with the Hermite function are done by a symbolic and algebraic manipulation language. Then a vector recurrence equation for  $n=0, 1, 2, \dots$  is obtained as

$$\frac{d}{d\tau} \mathbf{a}_n(\tau) = \underline{F}_n^{(-3)} \mathbf{a}_{n-3} + \underline{F}_n^{(-1)} \mathbf{a}_{n-1} + \underline{F}_n^{(0)} \mathbf{a}_n + \underline{F}_n^{(1)} \mathbf{a}_{n+1}, \quad (A2)$$

where

$$\mathbf{a}_n(\tau) = [a_n^0(\tau), a_n^1(\tau), a_n^2(\tau), \dots], \quad (A3)$$

and the  $\underline{F}_n^{(k)}$ 's are the coefficient matrices whose elements are listed elsewhere. Next, the reduced vector

$$\mathbf{b}_n(\tau) = \begin{bmatrix} \mathbf{a}_{3n}(\tau) \\ \mathbf{a}_{3n+1}(\tau) \\ \mathbf{a}_{3n+2}(\tau) \end{bmatrix} \quad (A4)$$

is shown to obey a tridiagonal vector recurrence equation:

$$\frac{d}{d\tau} \mathbf{b}_n(\tau) = \underline{\mathbf{M}}_n^- \mathbf{b}_{n-1} + \underline{\mathbf{M}}_n \mathbf{b}_n + \underline{\mathbf{M}}_n^+ \mathbf{b}_{n+1} \quad (n=0,1,2,\dots) \quad (\text{A5})$$

which have the following properties:

$$\underline{\mathbf{M}}_0^- = 0, \quad (\text{A7a})$$

$$(\underline{\mathbf{M}}_0)_{0j} = 0, \quad j=0,1,2,\dots, \quad (\text{A7b})$$

Here the coefficient matrices  $\underline{\mathbf{M}}_n$  and  $\underline{\mathbf{M}}_n^\pm$  are given by

$$\underline{\mathbf{M}}_n^- = \begin{pmatrix} \underline{F}_{3n}^{(-3)} & 0 & \underline{F}_{3n}^{(-1)} \\ 0 & \underline{F}_{3n+1}^{(-3)} & 0 \\ 0 & 0 & \underline{F}_{3n+2}^{(-3)} \end{pmatrix}, \quad (\text{A6a})$$

$$\underline{\mathbf{M}}_n = \begin{pmatrix} \underline{F}_{3n}^{(0)} & \underline{F}_{3n}^{(1)} & 0 \\ \underline{F}_{3n+1}^{(-1)} & \underline{F}_{3n+1}^{(0)} & \underline{F}_{3n+1}^{(1)} \\ 0 & \underline{F}_{3n+2}^{(-1)} & \underline{F}_{3n+2}^{(0)} \end{pmatrix}, \quad (\text{A6b})$$

$$\underline{\mathbf{M}}_n^+ = \begin{pmatrix} 0 & 0 & 0 \\ 0 & 0 & 0 \\ \underline{F}_{3n+2}^{(1)} & 0 & 0 \end{pmatrix}, \quad (\text{A6c})$$

$$(\underline{\mathbf{M}}_n^+)_{0j} = 0, \quad n, j=0,1,2,\dots \quad (\text{A7c})$$

When  $\mathbf{b}_0^{\text{st}}$  is given, the stationary solution  $\mathbf{b}_n^{\text{st}}$  of the recurrence equation of motion (A5) is obtained in the form of

$$\mathbf{b}_n^{\text{st}} = \underline{\mathbf{S}}_{n-1} \underline{\mathbf{S}}_{n-2} \cdots \underline{\mathbf{S}}_1 \underline{\mathbf{S}}_0 \mathbf{b}_0^{\text{st}}, \quad n=1,2,\dots, \quad (\text{A8})$$

where matrix  $\underline{\mathbf{S}}_n$  is introduced by  $\mathbf{b}_{n+1} = \underline{\mathbf{S}}_n \mathbf{b}_n$  for  $n=0,1,2,\dots$ . These are represented in the MCF form of  $\underline{\mathbf{M}}_n$  and  $\underline{\mathbf{M}}_n^\pm$  in the downward iteration

$$\begin{aligned} S_n &= -(\underline{\mathbf{M}}_{n+1} + \underline{\mathbf{M}}_{n+1}^+ \underline{\mathbf{S}}_{n+1})^{-1} \underline{\mathbf{M}}_{n+1}^- \\ &= - \frac{1}{\underline{\mathbf{M}}_{n+1}^- - \underline{\mathbf{M}}_{n+1}^+ \frac{1}{\underline{\mathbf{M}}_{n+2}^- - \underline{\mathbf{M}}_{n+2}^+ \frac{1}{\underline{\mathbf{M}}_{n+3}^- - \underline{\mathbf{M}}_{n+3}^+ \frac{1}{\underline{\mathbf{M}}_{n+4}^- \cdots \underline{\mathbf{M}}_{n+4}^+}}}} \underline{\mathbf{M}}_{n+1}^-, \end{aligned} \quad (\text{A9})$$

where  $1/\underline{\mathbf{M}}_k$  stands for inverse matrix  $\underline{\mathbf{M}}_k^{-1}$ .

Using the normalization condition  $[\mathbf{b}_0(\tau)]_0 = a_0^0(\tau) \equiv 1$ ,  $\mathbf{b}_0^{\text{st}}$  is determined by solving the simultaneous linear equation

$$\sum_{j=1}^{3P+2} (\underline{\mathbf{M}}_0 + \underline{\mathbf{M}}_0^+ \underline{\mathbf{S}}_0)_{ij} (\mathbf{b}_0^{\text{st}})_j = -(\underline{\mathbf{M}}_0 + \underline{\mathbf{M}}_0^+ \underline{\mathbf{S}}_0)_{i0}, \quad i=1,2,\dots,3P+2, \quad (\text{A10})$$

where a nontrivial solution exists because of  $|\underline{\mathbf{M}}_0 + \underline{\mathbf{M}}_0^+ \underline{\mathbf{S}}_0| = 0$ . Here we assume that the expansion and MCF are truncated as a suitable large integer  $p=P$  and  $n=N$ ; then the matrices  $\underline{\mathbf{M}}_n$ ,  $\underline{\mathbf{M}}_n^\pm$ , and  $\underline{\mathbf{S}}_n$  become  $(3P+3) \times (3P+3)$  square matrices. These truncation indices are determined by the requirement that further increases do not change the higher-order components, e.g.,  $a_0^1, a_1^1, \dots$ , within a given accuracy. It turns out that the scaling parameter  $\alpha$  influences crucially the truncation number  $P$ . The scaling parameter  $\alpha$  is determined in such a way that  $P$  and  $N$  become as small as possible. Typically, we choose  $\alpha \approx 2.0$ ,  $P=50$ , and  $N=50$ .

When we obtain the expansion coefficients  $a_n^p$ , any statistical properties in the stationary state can be calculated. For example, the distribution function is given by

$$W^{\text{st}}(u, \dot{u}) = \frac{1}{2\pi\alpha v_d(u)} \sum_{n=0}^{\infty} \sum_{p=0}^{\infty} \frac{a_n^p}{\sqrt{n!p!}} \exp \left[ -\frac{1}{2} \left[ \frac{u^2}{\alpha^2} + \frac{(\dot{u})^2}{v_d^2(u)} \right] \right] H_p \left[ \frac{u}{\alpha} \right] H_n \left[ \frac{\dot{u}}{v_d(u)} \right]. \quad (\text{A11})$$

Then, the intensity distribution function is determined only by  $a_0^p$  as

$$W^{\text{st}}(\bar{I}) = \frac{1}{\alpha\sqrt{2\pi}} \frac{1}{\bar{I}} \sum_{p=0}^{\infty} \frac{a_0^p}{\sqrt{p!}} \exp \left[ -\frac{1}{2\alpha^2} \left[ \ln \frac{\bar{I}}{A} \right]^2 \right] H_p \left[ \frac{1}{\alpha} \ln \frac{\bar{I}}{A} \right]. \quad (\text{A12})$$

From this expression, the stationary intensity moments  $\langle \bar{I}^n \rangle$  are given for  $n=1,2,\dots$  by

$$\begin{aligned} \langle \bar{I}^n \rangle &= \bar{A}^n \sum_{k=0}^{\infty} \sum_{m=0}^{\infty} \sum_{r=0}^m (-1)^r (2r-1)!! (2k+2m-2r-1)!! \frac{(n\alpha)^{2k}}{(2k)! \sqrt{(2m)!}} \begin{pmatrix} 2m \\ 2r \end{pmatrix} \\ &\times \left[ a_0^{2m} + \frac{n\alpha a_0^{2m+1}}{(2k+1)\sqrt{2m+1}} \frac{(2k+2m-2r+1)(2m+1)}{2k-2r+1} \right]. \end{aligned} \quad (\text{A13})$$

\*Present address: Nippon Telegraph and Telephone Corporation, Basic Research Laboratories, 3-9-11 Midori-cho, Musashino-shi, Tokyo 180, Japan.

<sup>1</sup>For instance, *Instabilities and Chaos in Quantum Optics*, edited by F. T. Arecchi and R. G. Harrison (Springer-Verlag, Berlin, 1987), and references cited therein.

<sup>2</sup>H. Haken, *Laser Theory*, Vol. XXV/2c of *Encyclopedia of Physics* (Springer-Verlag, Berlin, 1970); W. H. Louisell, *Quantum Statistical Properties of Radiation* (Wiley, New York, 1973).

<sup>3</sup>P. Jung, Th. Leiber, and H. Risken, *Z. Phys. B* **66**, 397 (1987); Th. Leiber, P. Jung, and H. Risken, *ibid.* **68**, 123 (1987); R. Graham, M. Hoehnerbach, and A. Schenzle, *Phys. Rev. Lett.* **48**, 1396 (1982); P. Jung and H. Risken, *Z. Phys. B* **59**, 469 (1985).

<sup>4</sup>M. Mörsch, H. Risken, and H. D. Vollmer, *Z. Phys. B* **49**, 47 (1982).

<sup>5</sup>P. Paoli, A. Politi, and F. T. Arecchi, *Z. Phys. B* **71**, 403 (1988).

<sup>6</sup>T. Ogawa, *Appl. Phys. B* **48**, 327 (1989).

<sup>7</sup>T. Ogawa, *IEEE J. Quantum Electron.* **QE** - **25**, 2169 (1989).

<sup>8</sup>C. O. Weiss and J. Brock, *Phys. Rev. Lett.* **57**, 2804 (1986); C. O. Weiss, N. B. Abraham, and U. Hubner, *ibid.* **61**, 1587 (1988).

<sup>9</sup>T. Ogawa, *Phys. Rev. A* **37**, 4286 (1988).

<sup>10</sup>T. Ogawa, *Jpn. J. Appl. Phys.* **27**, 2292 (1988).

<sup>11</sup>T. Ogawa, *Phys. Rev. A* **39**, 2264 (1989).

<sup>12</sup>E. N. Lorenz, *J. Atmos. Sci.* **20**, 130 (1963); H. Haken, *Phys. Lett.* **53A**, 77 (1975).

<sup>13</sup>T. Ogawa and E. Hanamura, *Appl. Phys. B* **43**, 139 (1987).

<sup>14</sup>T. Ogawa, *Appl. Phys. B* **49**, 397 (1989).

<sup>15</sup>S. Zhu, A. W. Yu, and R. Roy, *Phys. Rev. A* **34**, 4333 (1986);

M. Aguado and M. San Miguel, *ibid.* **37**, 450 (1988).

<sup>16</sup>L. W. Casperson, *J. Appl. Phys.* **46**, 5194 (1975); F. T. Hioe, *J. Math. Phys.* **19**, 1307 (1978); Yu. M. Ajvasjan, V. V. Ivanov, S. A. Kovalenko, V. M. Baev, E. A. Sviridenkov, H. Atomanspacher, and H. Scheingraber, *Appl. Phys. B* **46**, 175 (1988).

<sup>17</sup>H. Risken, *The Fokker-Planck Equation* (Springer-Verlag, Berlin, 1984), and references cited therein; H. Risken and H. D. Vollmer, *Z. Phys. B* **35**, 177 (1979); **39**, 89 (1980); **39**, 339 (1980).

<sup>18</sup>H. Risken, *Fortschr. Phys.* **16**, 261 (1968).

<sup>19</sup>Y. Yamamoto (private communication). This assumption is valid only in the case of the optical pumping by the number-state fields or the injection pumping via a high-impedance source. Quantum-mechanical treatment of the noise operators is found, e.g., in Ref. 2.

<sup>20</sup>Rigorous treatments of the adiabatic approximation in the Langevin equation are found in Ref. 17 and K. Kaneko, *Prog. Theor. Phys.* **66**, 129 (1981).

<sup>21</sup>H. A. Kramers, *Physica* **7**, 284 (1940).

<sup>22</sup>H. C. Brinkman, *Physica* **22**, 29 (1956).

<sup>23</sup>L. Mandel and E. Wolf, *Phys. Rev.* **124**, 1696 (1961).

<sup>24</sup>The general case  $T_{\text{obs}} \approx \tau_c$  of the good-cavity laser was studied in M. Lax and M. Zwanziger, *Phys. Rev. Lett.* **24**, 937 (1970).

<sup>25</sup>L. Mandel, *Proc. Phys. Soc.* **72**, 1037 (1958).

<sup>26</sup>*Handbook of Mathematical Functions*, edited by M. Abramowitz and I. A. Stegun (Dover, New York, 1972).

<sup>27</sup>H. Risken, H. D. Vollmer, and H. Denk, *Phys. Lett.* **78A**, 22 (1980).

<sup>28</sup>T. Ogawa (unpublished).